Carbon Sequestration in a Forest Area in Speulderbos, Netherlands

XING JIA
February, 2017

SUPERVISORS:
Dr. ir. Christiaan Van der Tol
Dr. ir. Chris Mannaerts

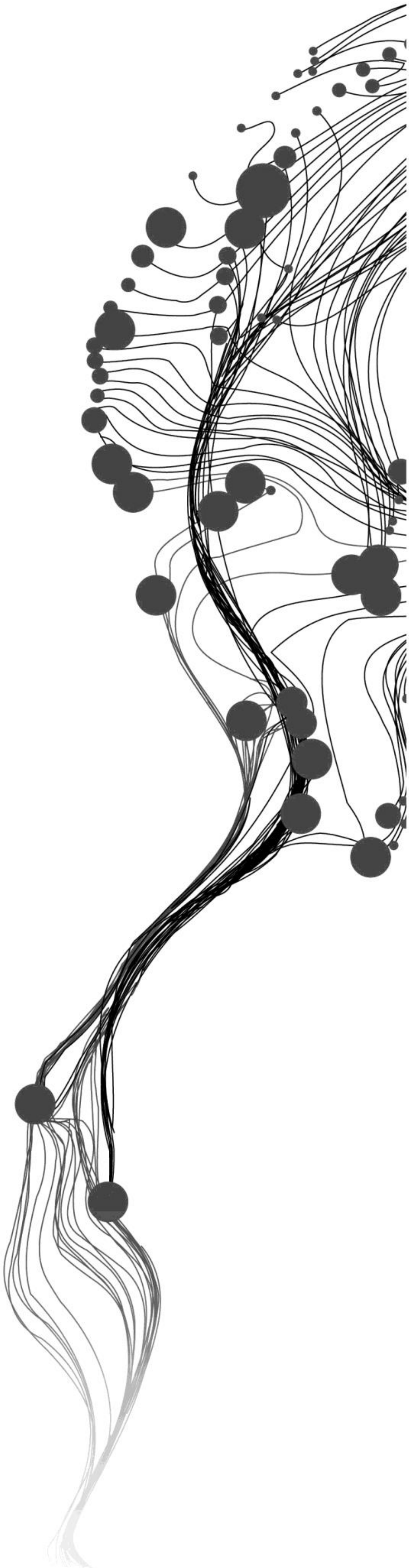

Carbon Sequestration in a Forest Area in Speulderbos, Netherlands

XING JIA
Enschede, The Netherlands, February, 2017

Thesis submitted to the Faculty of Geo-Information Science and Earth Observation of the University of Twente in partial fulfilment of the requirements for the degree of Master of Science in Geo-information Science and Earth Observation.
Specialization: Water Resources and Environmental Management

SUPERVISORS:
Dr. ir. Christiaan Van der Tol

Dr. ir. Chris Mannaerts

THESIS ASSESSMENT BOARD:
CHAIR: Dr. Ir. S. Salama
External: Dr. Ir.C.Shi

ABSTRACT

Global warming is currently one of the key issues in climate change research. Forests as one of the main terrestrial ecosystems, not only play an important role in maintaining the regional ecological environment, but play a huge contribution in the global carbon balance. The Speulderbos forest in the Netherlands is large forest areas consist of a dense 2.5 hector Douglas fir stand planted in 1962. It contains a 47.4m high flux tower within it. As turbulence observations are susceptible to external disturbances and do not provide large amounts of data, the average data coverage in a year is relatively low. Therefore to obtain the continuous data a robust and consistent gap filling method is required. Quality control of eddy covariance should include instrument and sensor problem testing. The eddy covariance method measures the net ecosystem exchange. However, particularly for CO_2 exchange a lot more understanding of the ecosystem is gained, when the net flux is partitioned into the main components: gross carbon uptake and ecosystem respiration. The current research is aimed at quantifying the CO_2 fluxes using eddy covariance flux measurement system installed at, Speulderbos forest, Netherlands. The study mainly focusses on flux portioning, estimation of daily productivity of the forest, analysis of the tower footprint and how it is influenced by wind direction and velocity.

We show that the good data (flags 1 to 8) accounted of 61% and 58%, in 2015 and 2016 respectively. The cumulative of NEE is -1.567 g m^{-2} and the peak is -1.570 g m^{-2} in 2015. Cumulative of NEE is -1.747 g m^{-2} and the peak is -1.752 g m^{-2} in 2016. The average daily GPP for 2015 is 20.15 g m^{-2} d^{-1}, 2016 is 22.38 g m^{-2} d^{-1}. And 9.26 % of the footprint was in the Douglas fir.

Keywords: *eddy covariance, net ecosystem exchange, gross primary productivity, footprint*

ACKNOWLEDGEMENTS

First of all, my deepest thanks to my parents for their honourable support, encouragement and love. Thanks for the joint efforts of ITC and Resources Environment and Tourism College of CNU to offer me this great opportunity to study at the Water Resources and Environment Management department. Both of the departments provide excellent academic environment for their students and staff in the spirit of science and humanity.

Especially gratitude to Dr.Christiaan Van der Tol, whom I cannot make it in my research without. I appreciate the tremendous patience and help throughout the whole research period he provided to me.

To my second supervisor, Dr. Chirs Mannaerts, for his useful comments and advises that encouraged me during the entire period of my pursuance of the thesis. Without their enlightening instruction, impressive kindness and concern, I could not have completed my thesis. Their keen and vigorous academic observation enlightens me not only in this thesis but also in my future study.

I shall extend my thanks to all my friends and classmates, our 6 member team from Capital Normal University, for all their kindness and caring. I would also like to thank all my classmates who have helped me to finish this thesis, especially Ceasr, Vikas Pingle and Mutinda Mbatha.

Finally, I would like to thank Andre Foeken, thank you for giving me a lot of encouragement and support, let my Dutch life has become colorful.

Dan je wel dat je er altijd voor me bent.

TABLE OF CONTENTS

LIST OF FIGURES

LIST OF TABLES

1. INTRODUCTION

1.1. Background

Global warming is currently one of the main topics of global climate change research. In 2007, the report of the Intergovernmental Panel on Climate Change (IPCC) stated that global warming of the climate system is an indisputable fact. This phenomenon is likely to be caused by an increase in greenhouse gas concentrations due to human activities (Yu & Huang, 2008). If no action is taken, human-induced climate change is likely to bring some "abrupt and irreversible" consequences. Numerous studies show that the terrestrial ecosystem is an important sink. It plays a key role of carbon to reduce global imbalances (Yang & XingWang, 2001). Forests as the main terrestrial ecosystems, it not only plays an important role in maintaining the regional ecological environment, but also in the global carbon balance plays a huge contribution.

Houghton JT et al. (2001) present Global forest area accounts for 27% of the land area, but store more than 80% of the global land carbon stocks and about 40 % of global soil carbon storage. The total amount of carbon stored in forest ecosystems is 854-1505 Gt, sequestrated carbon per year represents about 2/3 of terrestrial ecosystems (Kramer, 1981). Field, Raupach, & Victoria, (2003) also demonstrated that forests store near half of terrestrial carbon, make almost 50% contribution of terrestrial net primary production.

Nowadays, Forest carbon cycle research methods are plots inventory method, model simulation, GIS technology and eddy covariance method (Ying, 2005). Plot inventory method is a typical plot of harvesting method It accurately determinate of forest ecosystems through the establishment of vegetation, litter or soil carbon storage, and can be obtained flux through a certain period of continuous observation (Fang, Chen, Peng, Zhao, & Ci, 2001). Simulation model is to estimate productivity and carbon storage in forest ecosystems through mathematical models, mainly for large -scale forest ecosystem carbon cycling research. But some characteristic parameters of ecological processes are not readily available, and are difficult to grasp the availability of standards, so modeling is difficult (Ipcc Wg1, 2003). Earth Information technology is mainly used to make up for lack of model simulations, estimates of land use and land cover change on carbon storage (Jiyuan & Guirui, 2010). The eddy covariance method measures the vertical wind velocity and CO_2 mixing ration between the atmosphere and top of canopy. Now it is considered to be the most direct standard way to measure the energy and flux between the biosphere and the atmosphere (Bonan, 2008).

Eddy covariance measurement systems are currently the most preferred for quantification of turbulent fluxes, following their development over the last one and a half decade; especially because such systems can also be used to quantify CO_2 fluxes(Evans et al., 2012). With the eddy covariance technique development, now this method is becoming the popular way to assess ecosystem carbon exchange. There are three points that make it popular. Firstly, it provides a measurement at an appropriate scale to assess net CO_2 exchange of the whole ecosystem. Secondly, it produces a direct measurement across the interface between the canopy and the atmosphere. And in the study area sampled with this technique, called the flux footprint, possesses longitudinal dimensions ranging between a hundred meters and several kilometres (Schmid, 1994). Lastly, this method is capable of measuring the ecosystem exchange of CO_2 from hours to years, with a broad time scales (Asante-yeboah, 2010).

Flux estimates were contained a complete database when they were based on direct measurements, such as, net ecosystem production (NEP) which is a fundamental property of ecosystems. The difference between gross primary production and total ecosystem respiration (Reco) is defined as NEP. Net ecosystem exchange (NEE) was equal to –NEP, which was the sum of the eddy covariance CO_2 flux above the plant canopy. It represents the total amount of organic carbon in an ecosystem available for storage (Lovett, Cole, & Pace, 2006).A derived quantity is the gross primary production (GPP) which represents the gross uptake CO_2 that is used for photosynthesis, whereas, GPP was calculated from the NEE and calculated Reco.

This study is aimed at quantifying CO_2 fluxes using flux measurements taken by an eddy covariance system installed in the forest area, Speulderbos, Netherlands. Specifically, it will focus on flux portioning, estimate the daily productivity of the forest; and shall involve analysis of the tower footprint and how it is influenced by wind direction and velocity.

1.2. Objectives

1.2.1. Problem definition

By sequestering large amounts of atmospheric carbon, forests play an important role in the global carbon cycle (Schimel et al., 2001). In the case of Speulderbos forest, there is located an eddy covariance flux tower in it. Around the flux tower the mainly plant is Douglas fir. There is few study of flux partitioning at this site. The quality control of the raw data has been poor until now. The effect of the different forest stands nearby on the measured flux at the tower is unknown. The present MSc studies will address a number of specific questions as phrased below. Base on this study, it will provide a reference for research in forests area.

1.2.2. Main objective

To quantify the gross and net CO_2 flux in a forest area in Speulderbos, Netherlands.

1.2.3. Specific objectives

To obtain and pre-process the flux tower data of flux tower measurement between 2015 and 2016.

To calculate the CO_2 flux using the eddyUH software.

To quality control the CO_2 flux data using the Vickers & Mahrt (1997) method.

To separate the CO_2 flux data using Reichstein et al.(2005) flux partitioning model.

To analyze the effect of wind direction and velocity on tower footprint and obtain the footprint maps from the flux data.

Estimate the daily primary productivity of the forest between 2015 and 2016.

1.3. Research Questions

After filtering for quality according to Vickers & Mahrt (1997), what was the percentage of high quality data?

How much was the GPP in 2015 and 2016?

What is the effect of wind direction and speed on the tower footprint?

Can the flux be separated into a flux from the Douglas fir and from other forest types by analyzing the footprint area?

2. LITERATURE REVIEW

2.1. Software for analysis of flux tower processes

With the eddy covariance method development, the majority of scientific groups use their own software to achieve their specific objectives. Even though researchers write their own software to process specific data, recently, comprehensive data processing packages have become available from flux networks, research groups and instrument manufacturers.

There are several examples:

EdiRe (developed by Dr. Robert Clement at the University of Edinburgh) is a fast, flexible software tool for micrometeorologists, focus on eddy covariance and microclimatic analysis. EdiRe is suitable for most eddy covariance raw data formats and is able to incorporate microclimatic data. The graphical user interface simplifies the development of handlers and allows quick redesign of the program to enhance the data analysis question/answer cycle.

EddyPro (developed by LI-cor, Lin-coln, NE) is for processing raw eddy covariance (EC) data to compute biosphere/atmosphere fluxes of CO_2, H_2O, CH_4, other trace gases, and energy. EddyPro is to efficiently process eddy covariance data logged to gas analysers (.ghg files). It is designed to provide easy, accurate EC flux computations. It also supports other raw file types, including data stored as ASCII tables, binary files, and SLT formats.

Alteddy (developed by Alterra) is software which can view raw data, calculate normalized spectra and cospectra, and convert raw binary files to ASCII files, calculate planar fit coefficients, calculate solar elevation and radiation, check the site coordinates in Google Maps. It can handle major instruments and ASCII, binary, and so on data formats.

EddyUH (developed by University of Helsinki) is a open software package. It is written by the Matlab and has a convenient graphical user interface EddyUH can process data from a variety of different combinations of sonic anemometers and gas analysers and from a variety of different measurement locations. The software can process temperature, CO_2, H_2O, CH_4, N_2O, O_3 and particulate high frequency data. It includes the latest updated corrections and methods for EC flux estimation.

2.2. Eddy Covariance of the CO_2 flux

The general principle of Eddy Covariance measurements is covariance between the concentration of interest and vertical wind speed in the eddy. As George Burba (2013) present in turbulent flow, flux is equal to a mean product of air density (pd), vertical wind speed (w), and the mixing ratio(s) can be presented as:

$$\mathrm{F} = \overline{\mathrm{p_d ws}}$$

……Equation 1

The right hand side of above equation can be broken down into means and deviations. Assuming air density fluctuations and mean vertical flow in the horizontal homogenous terrain are negligible. Finally, the Eddy Flux equation will get:

$$\mathrm{F} \approx \overline{\rho_{\mathrm{d}} w' s'}$$

……Equation 2

In the above equation, ′ means deviations from the mean.

2.3. Data quality control

Quality control of eddy covariance measurements does not exist a uniform program. Only few aspects are discussed in the papers.

Vickers & Mahrt (1997) argue that the basic testing of the raw data is the first step in data analysis such as electrical tests of the amplitude, resolution of signal, control of the electronic and meteorological ranges of data and spikes (Hojstrup, 1993).Time series sampling errors apply for statistical tests (Finkelstein & Sims, 2001).An important part for quality control are tests on fulfilment of the requirements for eddy covariance measurements. Foken et al. (2004) present a system of general quality flagging of the data. It gives a set of possible tests and protocol for data flagging for continuously running eddy covariance systems.

Foken classification system (Foken et al., 2004) which separate three types: Steady state test condition associated with the vertical wind speed and CO_2 concentration; Integral turbulence characteristics; Horizontal orientation of the sonic anemometer.

2.4. Gap filling

Some raw data because of equipment failure or the harsh environment were missing, while other raw data were implemented in the quality control processes. Then the missing data need to be gap filled.

Numerous filling methods for NEE have been used by others. Studies on the effects of filling methods for energy fluxes on calculated annual sums have been reported (Falge, Baldocchi, Olson, Anthoni, Aubinet, et al., 2001). Long term records of energy fluxes are typically constructed on coarser time scales (months) using, for example, the water balance equation for λE and estimating the residual H as an energy balance equation (Jaeger & Kessler, 1997). In Falge, Baldocchi, Olson, Anthoni, Aubinet, et al. (2001), gap filling method based on the concepts of mean diurnal variations and look-up tables for filling. It is emphasized that it is import to standardize the method of data post-processing phase, as annual sums of energy fluxes resulting from the selected methods are not necessarily compatible with each other.

2.5. Flux portioning

The eddy covariance method measures the net ecosystem exchange (NEE). However, particularly for CO_2 exchange a lot more understanding of the ecosystem is gained, when the net flux is partitioned into the main components: gross carbon uptake (GPP) and ecosystem respiration (Re).GPP is defined as:

$$\mathrm{NEE} = \mathrm{GPP} - \mathrm{Re}$$

……Equation 3

Where Re is the ecosystem respiration, it is temperature dependent. According to the annual Q10 method, it can be calculated as:

$$\mathrm{Re}_{\mathrm{AQ10}} = \mathrm{R}_{10}\mathrm{Q}_{10}^{(\mathrm{TA}-10)/10}$$

……Equation 4

Where R10 is base Re at a reference temperature, here 10℃, and Q10 describes the exponential temperature response of Re.

Reichstein et al., (2005)suggested that the parameters of Annual Q10 method may vary along the annual cycle, and advised a tactics by which the parameter values of the base respiration and the temperature response can be estimated over the time scales at which they might vary using the 'short-term exponential' (STE) method. They used the Arrhenius, (1889)equation after Lloyd & Taylor,(1994):

$$\mathrm{Re}_{\mathrm{STE}} = \mathrm{R}_{10,\mathrm{STE}} \exp(\mathrm{E}_0 \left[\frac{1}{283.15 - \mathrm{T0}} - \frac{1}{\mathrm{Ta} - \mathrm{T0}}\right])$$

……Equation 5

with a constant T0 parameter (227.13 K, Lloyd and Taylor, 1994) and a 15-day moving window to determine variability in the temperature sensitivity parameter (E0), then a 4-day window to estimate the base respiration parameter (R10,STE)(Reichstein et al., 2005).

2.6. Footprint calculation

Footprint is a relative contribution of each point to the measured flux (or concentration).Footprint is strongly associated with receptor height, atmospheric stability, and surface roughness. Lagrangian stochastic models or large-eddy simulation computation cost much time and cannot readily be applied for long-term measurement programs. Kljun, Calanca, Rotach, & Schmid,(2003) present a scaling procedure for flux footprint model, a simple parameterization for the scaled footprint estimate. This method can be applied to any given stability condition. Kljun, Calanca, Rotach, & Schmid, (2015) present a modified method: Two dimensional parameterization for Flux Footprint Prediction (FFP). FFP now provides not only the range of footprint estimation but also the width and shape of footprint estimate, and the effect of surface roughness length. Parameterization is valid for a wide range of boundary layer conditions and measurement altitudes across the planetary boundary layer. Therefore, it can provide footprint estimation for a wide range of practical applications.

3. DATA

3.1. Study Area description

The Speulderbos forest is a large forest area in the Netherlands. It is located at 52°15'18"N, 5°41'25"E, and 52m amsl. A 47.4m high flux tower within a dense 2.5 ha Douglas fir stand planted in 1962. Douglas fir presented a trapezoidal shape. *Larus kaempferi, Fagus sylvatica, Pinus sylvestris* and *Tsuga spp* are the dominant species near the Douglas fir plantation. At a distance of 1,500 meters from the eastern part of the tower, the forest is connected to the large heather area. In all other directions, the vegetation consists of a few kilometres of forest(Raj, Hamm, van der Tol, & Stein, 2014). The displacement height is 18m. The boom direction is around 275° .The roughness length is about 1.27. The topography of flux tower is lightly undulating with height of 10m to 20m around distance of 1km (Su et al., 2009). The altitude is 60m (a.s.l). Terrain slightly ups and downs, in the distance of 1000 meters height change of 10-20 meters. The location of the study area is shown in Figure 1.

Figure 1 Overview of Speulderos

3.2. Instrumentation

At this study area, at the top of scaffolding tower (47.4 m) installed eddy covariance and radiation measurements. Above the canopy crown (30m) other meteorological measurements are carried out. In the different canopy components contact the temperatures (from 20 to 32m height), and at ground level (Su et al., 2009).

3.3. Data Requirements

To analyse the behaviour of carbon sequestration in Speulderbos, the CO_2 flux was calculated by the software eddyUH, the gross primary productivity will be portioned by the Reichstein et al (2005) method, the effect of wind direction and velocity on tower footprint and the footprint map will be simulated by the Kljun et al (2015) method.

3.3.1. Flux calculation Data

Flux data and meteorological data need to be processed which includes sonic wind speed and sonic temperature were measured by the Campbell CSAT 3, relative humidity, air temperature, air pressure and so on. Those data are measured by the filed instruments.

The flux data are saved as generic ASCII-flies which from 2015/03/26 to 2016/09/11. The meteorological data is from 2015/06/17 to 2016/08/29.

Table 1 Data Used for Flux Calculation

U [m s^{-1}]	Sonic Wind speed u
V [m s^{-1}]	Sonic Wind speed v
W [m s^{-1}]	Sonic Wind speed w
TS [Celsius]	Sonic Temperature
RH [%]	Relative Humidity
Ta [Celsius]	Air Temperature
Pre [hpa]	Air Pressure

3.3.2. Flux Partitioning Data

To portion the CO_2 flux, the use of correct high quality data is the key to success. The net ecosystem exchange (measured by the Licor 7500), radiation global, friction velocity which calculated by the eddyUH, time series and meteorological variable are got from the filed measurement.

The radiation global is from 2015/03/26 to2016/02/27.

Table 2 Data Used for Flux Partitioning

NEE [μ mol^{-2} s^{-1}]	Calculated by eddyUH
LE [W m^{-2}]	Calculated by eddyUH
H [W m^{-2}]	Calculated by eddyUH
Rg [W m^{-2}]	Got from measurement
Tair [℃]	Air Temperature
rH [%]	Relative humidity
VPD [hPa]	Calculated it at Tair
Ustar [m s^{-1}]	Calculated by eddyUH

3.3.3. Footprint Data

To analyze the wind speed and velocity on tower footprint and obtain the footprint maps from the flux data, the fellow data is necessary.

Table 3 Data Used for Footprint

Zm [m]	Measurement height above displacement height
z0 [m]	Roughness length [m]
umean[m s^{-1}]	Mean wind speed at zm [m/s]
h	Boundary layer height
ol[m]	Obukhov length
sigmav [m s^{-1}]	Standard deviation of lateral velocity fluctuations [m/s]
Ustar [m s^{-1}]	Friction velocity [m/s]
Wind direction	Wind direction in degrees (of 360) for rotation of the footprint

4. RESEARCH METHODOLOGY

4.1. Methodology Flowchart

Figure 2 shows a flowchart of the overall methodology. The raw turbulent data, meteorological data, wind speed and direction, and remote image as a input data. First, the raw data and meteorological data were calculated by the pre-processing software eddyUH to calculate the net ecosystem exchange (NEE). The NEE was used for quality control thorough Vickers method or combined with wind speed direction and remote image to calculate the footprint. After doing the quality control, the high quality data were obtained, but at the same time the data gap will increase. Through the Falge gap filling method, the consecutive data is available. Consecutive data were performed flux partitioning with the method of Reichstein, after which gross primary productivity is available. The daily primary productivity can be estimated by aggregation of the fluxes over the day.

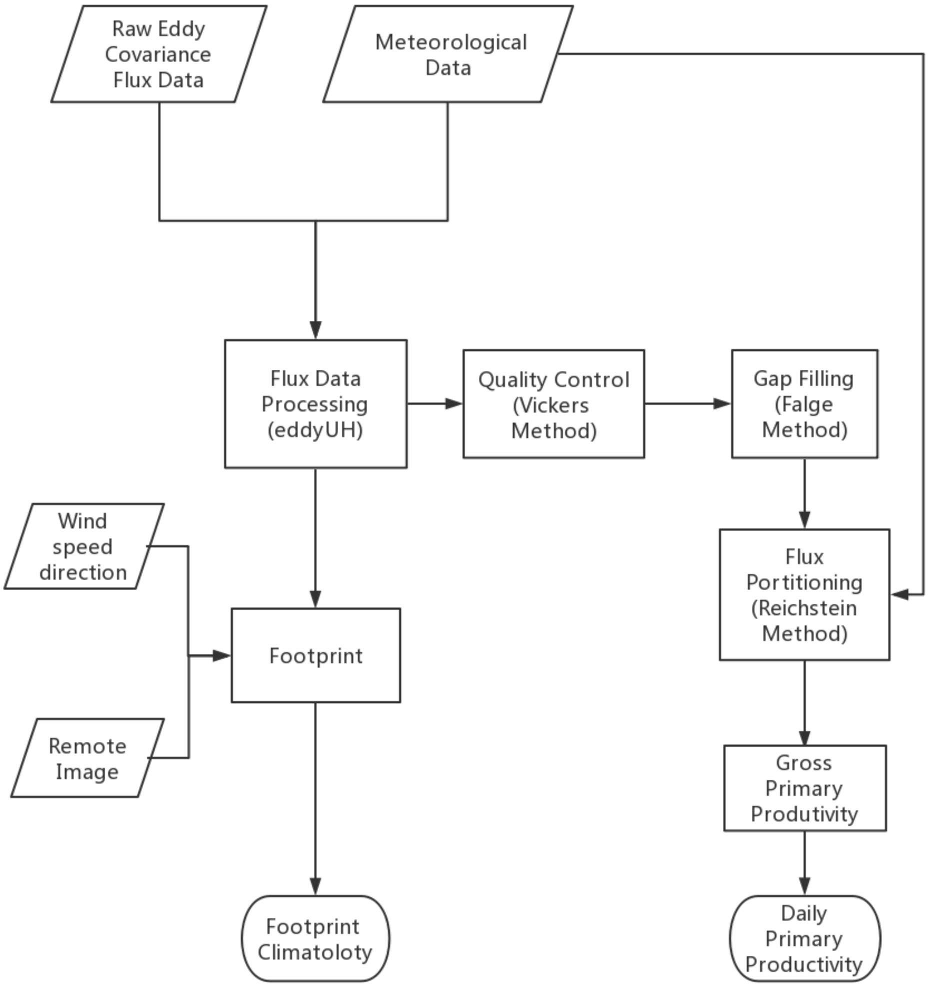

Figure 2 Methodology Flowchart

4.2. Raw Data Pre-processed

The raw data which were measured by the eddy covariance instruments require pre-processing, due to the fact that eddyUH only supports raw data files of a length of minutes is 30 minutes. The raw data were clipped to 30 minutes time length in text-files through the Matlab code.

4.3. Flux Calculation

The pre-processed data were used to for flux calculation through the eddyUH. eddyUH is the eddy covariance data post-processing software.

The turbulent fluxes of CO_2, sensible heat flux and latent heat flux are all of calculated through the relationship of covariance between respective scalar and vertical wind velocity, as below formula:

$$\mathrm{Fco_2} = \frac{\rho_\mathrm{d}}{\mathrm{M_a}} \overline{w'x_{CO2}'}$$

……Equation 6

$$\mathrm{H} = \rho_d c_p \overline{w'T'}$$

……Equation 7

$$\mathrm{LE} = \rho_d L_v \frac{M_w}{M_a} \overline{w'x_{H2O}'}$$

……Equation 8

In the formula, ρ_d represents the dry air density (kg m^{-3}), c_p is the specific heat capacity of dry air (J $kg^{-1}K^{-1}$), Lv represents the latent heat of water vaporize (J kg^{-1}), T the temperature (in the K)and Ma and Mw are the molar mass of the dry air and water, respectively. The term $\overline{w'T'}$, $\overline{w'x_{CO2}'}$and $\overline{w'x_{H2O}'}$ represent the w and T, dry molar fractions of CO_2 and H_2O the relationship of covariance. Overbars and primes are the value averaging and fluctuations, respectively.

Before using eddyUH to calculate turbulent fluxes, a 'project' was set: Metadata of the site environment and the basic information about the instruments were provided as input to eddyUH. As the Mammarella, Peltola, Nordbo, Järvi, & Rannik, (2016) note, different software packages are available, but the methods are the same for the most steps. In this thesis, as mentioned section of above, eddyUH was used to process the data. However, the estimated fluxes still showed some differences depending on the software that was used due to the flux corrections, even though the preparation and processing steps of the raw data were consistent in both software packages. In the open-path systems the most critical step is the density correction. This will be explained in further detail below.

The project contains four main parts: file information, measurement system, site description, post-processing methods.

4.3.1. File Information

In this part, raw data and meteorological data were major input. Due to the meteorological data were only available for the period between 2015/03/26 and 2015/06/17, virtual meteorological data were used outside this period. These data are assumed by the eddyUH based on the site location and daytime. From the below section, it can obviously found that air temperature reality humidity such meteorology data can easily affect the turbulent fluxes calculation. Besides, the meteorology data were also used for the gap-filling and flux partitioning. The gap-filling process, finds the same meteorological condition as in the gap, and uses the flux data at this condition to fill the gap. In flux partitioning process, the meteorology data such as air temperature, relative humidity, pressure directly participated in the calculation.

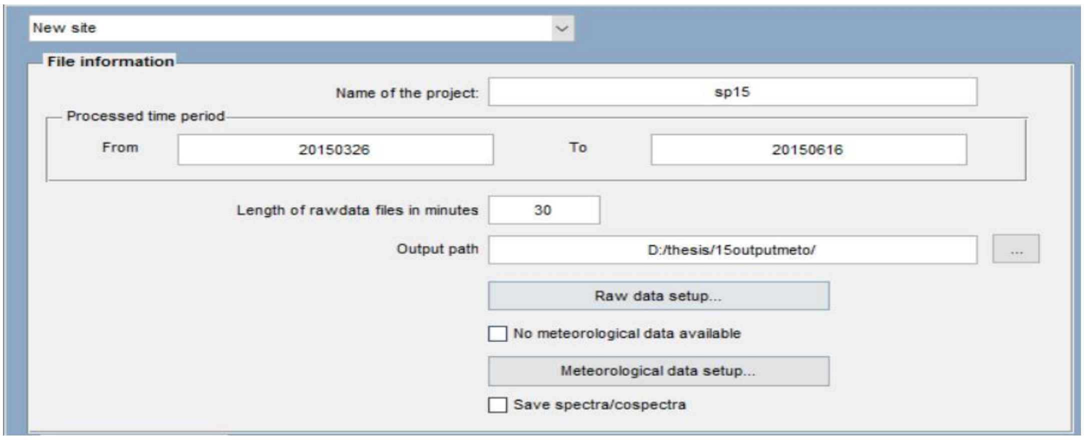

Figure 3 Scheme for File Information

4.3.2. Measurement system

The sonic anemometer and gas analyzers were settled in this part. The sonic anemometer name is Campbell CSAT3. The path length is 0.12m, time constant is 0.1s and sampling frequency is 20 Hz. The wind speed variables saved as m/s. The sonic temperature is saved in raw data as Celsius.

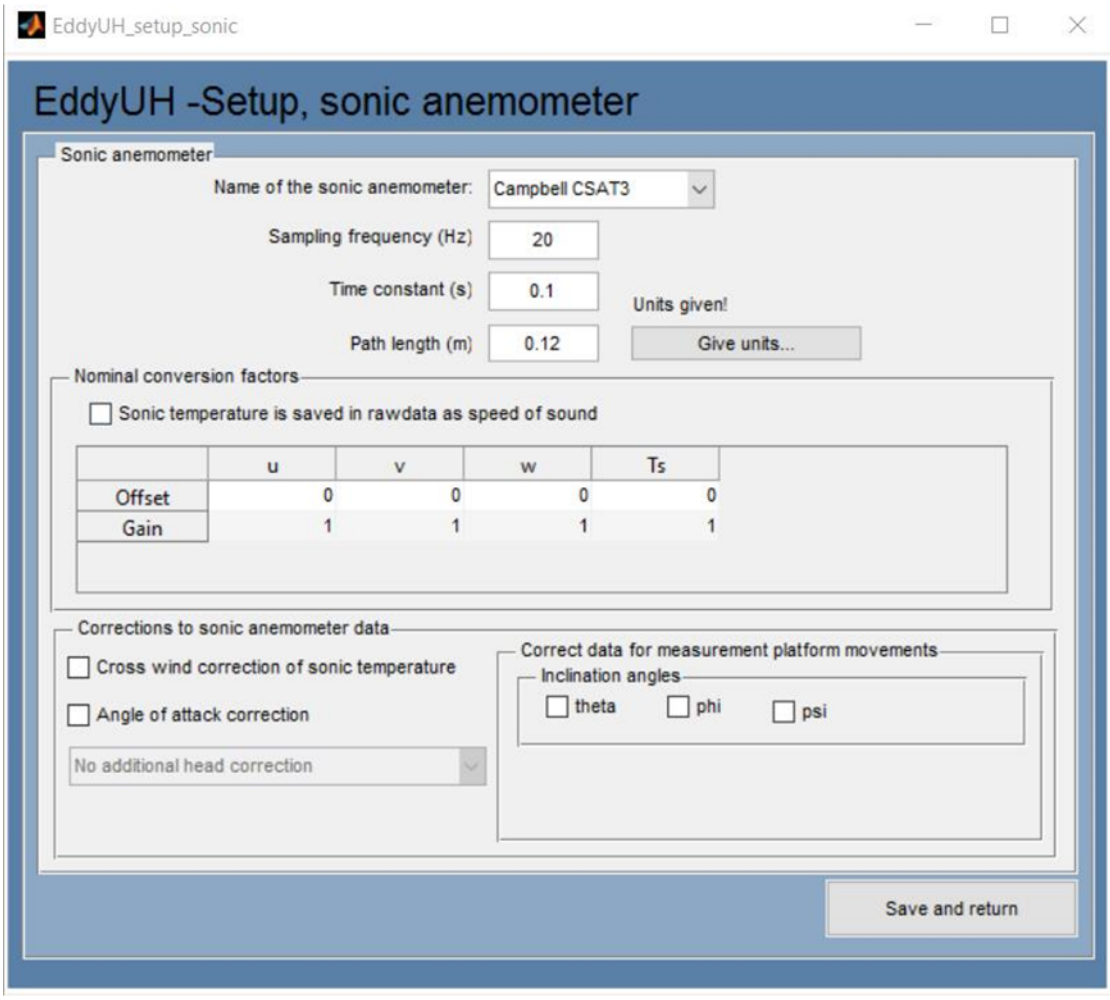

Figure 4 Scheme for Sonic anemometer

A Licor7500 gas analyser was used, which analyser the concentration of two variables, CO_2 and H2O. Following gas analyser characters settled as the path length is 0.12m, the gas analyser time constant is 0.1s and horizontal sensor separation 0.15m.

Due to the gas molar densities measured by the open-path analysers in the open measurement cell, if not properly corrected, the temperature and humidity fluctuations could cause apparent surface fluxes in the open cell. It is therefore needed to perform WPL- correction to the averaged fluxes to correct data for air density fluctuations. The WPL correction is often larger in magnitude than the original flux, and the flux may change sign after WPL correction(Peltola, Mammarella, Haapanala, Burba, & Vesala, 2013). With further academic research, more and more correction method have been introduced in the literature, and application of these methods demonstrate that the magnitude of the corrected fluxes increase. It is therefore critical to perform such corrections accurately, especially when small fluxes of CO_2 occur with large H and LE fluxes. Lee & Massman (2011) showed that 2% error in H spectral corrections will result in 40 g (CO_2) m^{-2} bias annually. It proved that any bias in the correction term will led the WPL correction to bias the flux estimate. However, the WPL correction term implement correctly will not led to a bias of

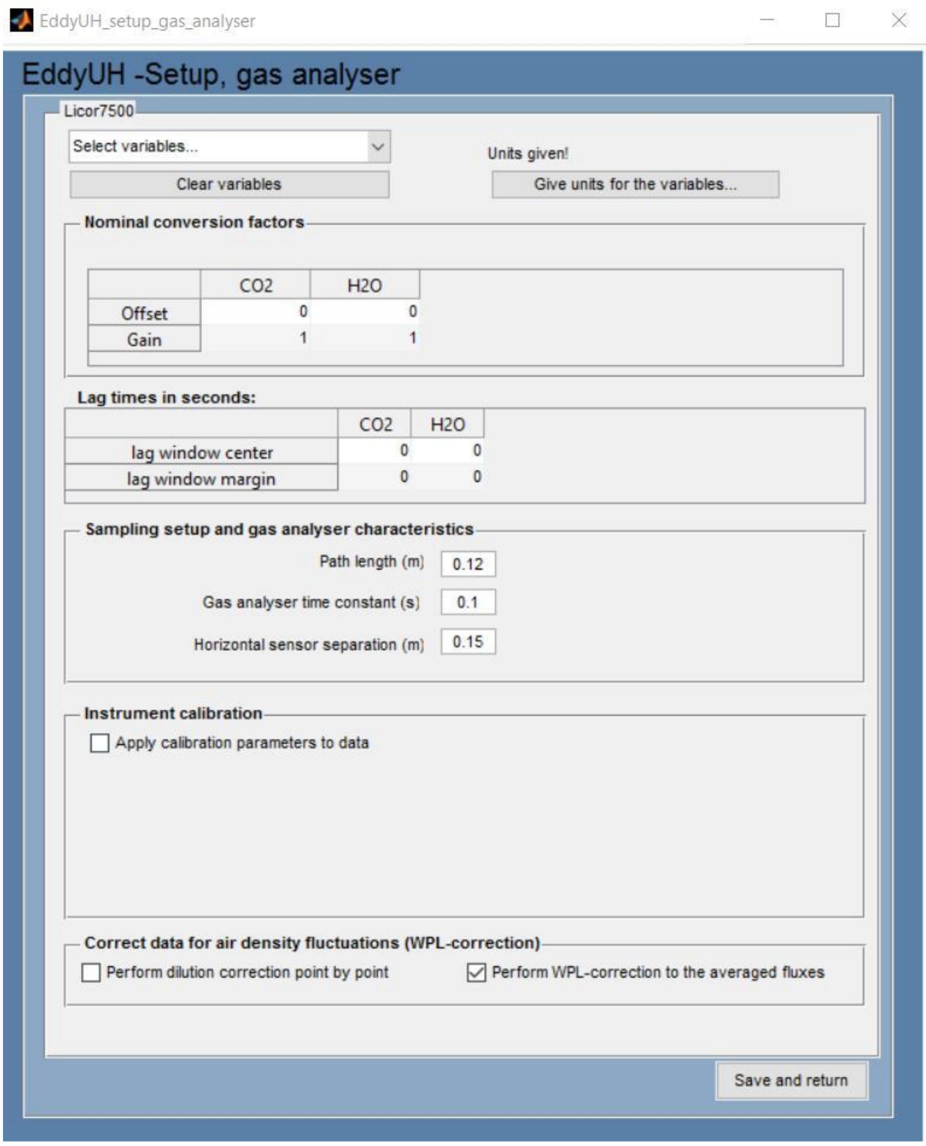

the resulting fluxes.

Figure 5 Scheme for Gas Analyser

4.3.3. Post-processing Methods

At first the post-processing methods have been defined. The averaging period is 30 minutes. A coordinate rotation is for the wind velocity, the purpose is to align the x-axis parallel to the mean wind direction and set the value of mean vertical velocity as zero. The common practice is 2D-coordinate rotation. The purpose of detrending is to extract the turbulent fluctuation from the measured time series through subtracting the mean part. The block-averaging term fulfils the Reynolds averaging rules. The block-averaging has the smallest effect on the cospectra (Rannik & Vesala, 1999). The despike method was used a lower and upper limits for values method. It has consistency limits for each data point, data exceeding the setup limits were marked as a spike and replaced with previous the value.

Then the column order of the data in raw data files was described in the input of eddyUH.

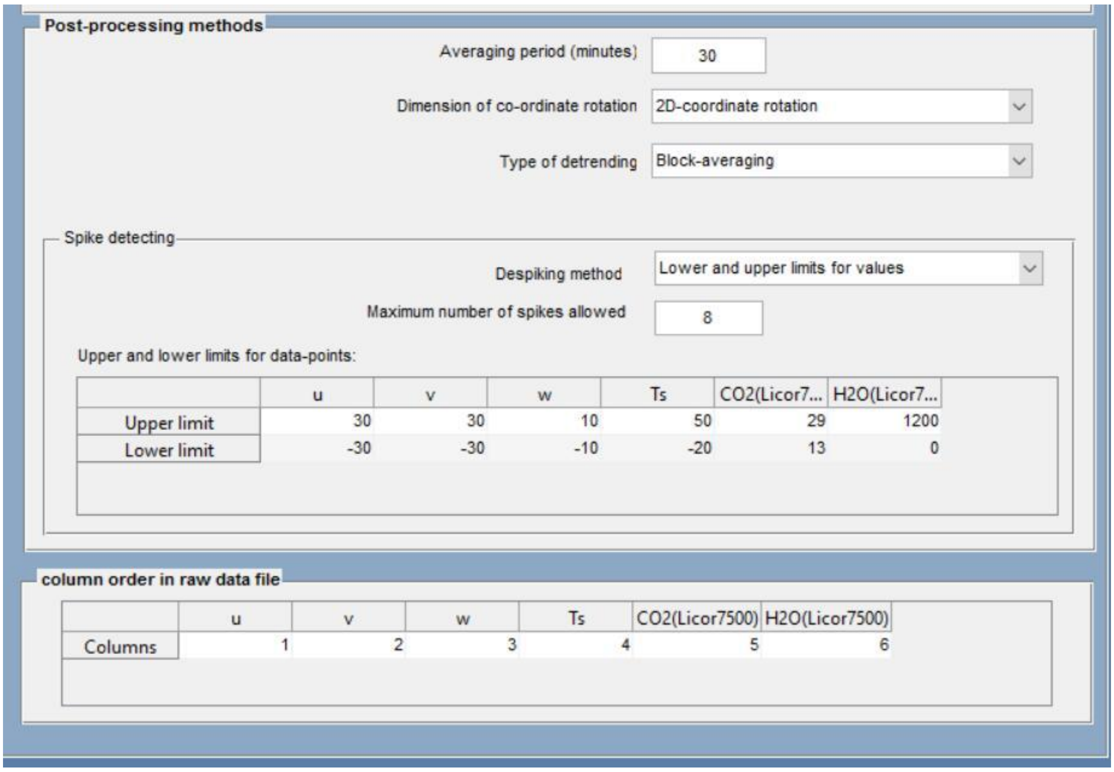

Figure 6 Scheme for Post-processing Methods

4.3.4. Calculate final fluxes

After the installing a project, eddyUH loads the raw data. The gap of raw data, in 2015 accounted for 9.88%, in 2016 accounted for only 1.44%. So the raw data availability satisfying for doing the flux calculation.

By default all variables listed in eddyUH are be saved in monthly ASCII-files, besides the interested variables could be saved in a separate files or figures.

At first, HORST (1997) method is used for scalar model cospectrum and cospectral peak frequency vs. stability parameterisation to do the spectral corrections.

Then, the methods of spectral correction are selected. The sonic anemometer fluxes (sensible heat and momentum fluxes) are always corrected by using HORST (1997) theoretical approach.

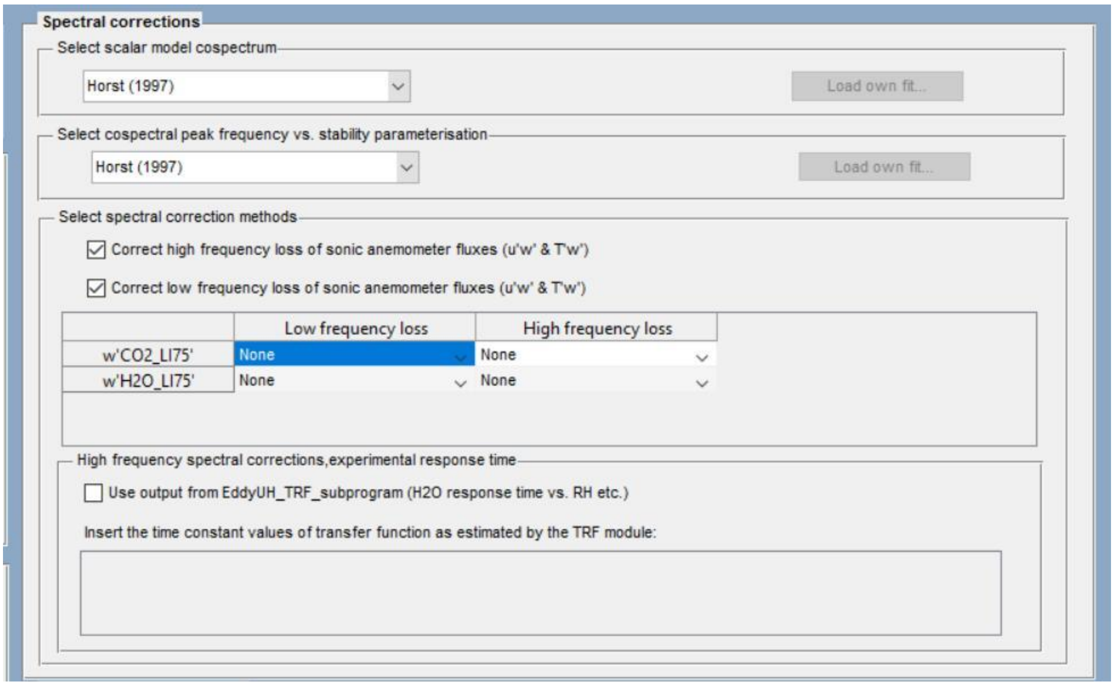

Figure 7 Scheme for Spectral Corrections

Finally, the standard method is used for of lag determination.

Besides, in the current version eddyUH, the flux quality flags are not used, and the 30 min flux values, which do not pass any of the chosen quality criteria are removed and replaced with missing value(-999). So the quality filtering was not chosen.

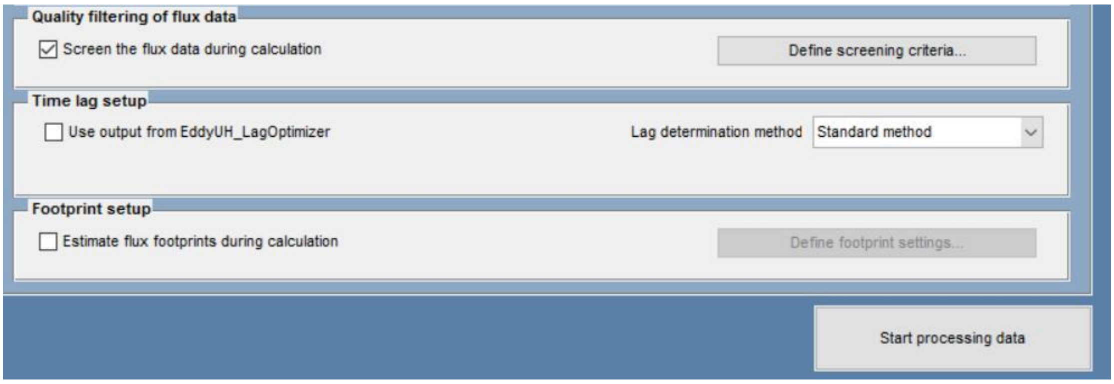

Figure 8 Scheme for Quality filter and Time Lag Setup

Finally, covariances were calculated by the eddyUH. The outputs include the mean, standard deviation, skewness, kurtosis statistic of wind and flux signals, power spectra and co-spectra of each time interval. All these output data are saved in monthly ascii-files.

4.4. Flux Partitioning

4.4.1. Gap-filling

The eddy covariance method presents continuous data sets of turbulent flux and energy exchange between ecosystem and atmosphere. But, the gaps were annoying apparent due to severe weather and instrument failure. Thus a standardized gap filling for those gaps is necessary.

In this thesis, the gap filling of the eddy covariance and meteorological data is based on the Falge, Baldocchi, Olson, Anthoni, & Aubinet (2001), but also considering the fluxes co-variation and variables of meteorological and the fluxes temporal auto-correlation(Reichstein et al., 2005).

In this method, three different conditions are identified:

Table 4 Three Conditions of Gap Filled Case

case	solution
Missing the direct interest data, but the meteorological data are available.	Missing data will be replaced by the value under the same meteorological environment (Rg±50W m^{-2}, Tair±2.5℃,VPD±5.0hPa) at 7 days' time-windows. If no same meteorological condition, it will increase to 14 days.
Missing the direct interest data, and Tair (air temperature) or VPD (vapor pressure deficit) missing, but Rg (radiation global) is available.	Use the same approach like case 1, but the same meteorological only is treated as Rg less the bias 50W m^{-2}. In addition, the time-windows cannot increase.
Missing the direct interest data, Tair or VPD and Rg	Missing data will be replaced by the value at the same time of the day(±1h)

If after those steps the value could not find it, it will be enlarge the time-windows until it can be replaced.

The filled data will be classified into different level (A, B, C) based on the different case (1, 2, 3) and time-windows size used as Figure 9 .

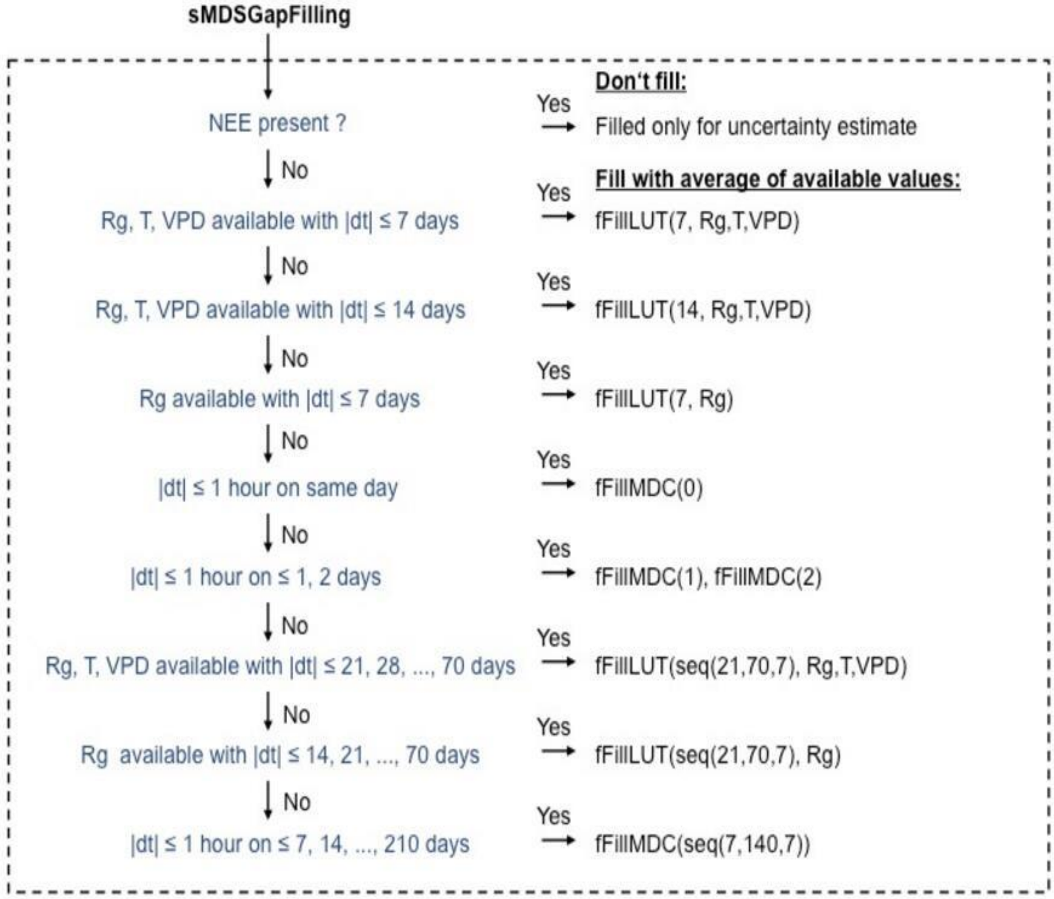

Figure 9 Flow Diagram of the Gap-Filling Algorithm source: Reichstein et al.(2005)

4.4.2. Friction velocity (u*) threshold estimation

Stable ambient atmosphere and low turbulent fluxes, especially in the night or still air conditions, will lead to an underestimation of the night-time turbulent fluxes, such as ecosystem respiration. It can be detected by micro-meteorological quality control. In case where the necessary information for these tests can be obtained, the widely accepted method assumes that the threshold for the friction velocity (u*) can be the location and season at which the night-time flux is considered to be valid. This threshold is typically established by associating the night-time flux with the friction velocity, while treating the temperature as a covariate.

In this thesis, Papale et al. (2006) was used to estimate the minimum friction velocity. At first, it was necessary to define the season. At this method was designed to avoid breaks at year boundaries so as a continuous season as default. The seasons begin in March, June, September, and December as spring, summer, autumn and winter respectively. The annual friction velocity thresholds were then applied according to successive seasons across the year boundaries. If there is few numbers of records, before estimating the threshold of friction velocity, the data of seasons were be combined as one year. Then, Papale et al.(2006)method estimated the threshold at the similar friction velocity and compute mean NEE and mean friction velocity at each class (default 20 classes) in each season or temperature subclass. Moving point test was applied to each package to determine the threshold. The last, in this thesis, a bootstrap was used to estimate the uncertainty of the threshold. It will give 5%, 50%, 95% three levels as a range of the estimated threshold.

4.4.3. Data selection

The starting point of the flux partitioning analysis is the data selection. The raw data was used to estimate the reference temperature. The gap-filled data only was used for the partitioning step.

First, in order to filter ecosystem respiration (Reco) from night-time data, only half an hour was chosen with global radiation (Rg) less than 10 W m^{-2} and cross-checked with sunrise and sunset data derived from local time, and standard solar geometry routines calculated potential radiation. Next, the data set is divided into continuous periods of length x (defaults as 14 days), and in each periods more than six data points and temperature range is greater than 5℃ were available. Only under these conditions, a reasonable regression of Reco for the temperature can be expected.

4.4.4. Flux-partitioning algorithm

The flux partitioning algorithms follows four steps:

First, estimate the temperature from the seasonal data. As the Lloyd & Taylor (1994)exponential regression model said, the Reco data are related to the air temperature:

$$\mathrm{Reco} = \mathrm{Rref}e^{E0(1/(Tref-T0)-1/(T-T0))}$$

……Equation 9

While the T0 is a constant of -46.02 as in the Lloyd & Taylor (1994), the activation energy kind of parameter(E0), was allowed to a free parameter. And the reference temperature (Tref) is set to 15 ℃.

Second, the temperature sensitivity from short-term data was estimated. The short-term data temperature sensitivity estimated same as the seasonal data. The differences are the estimated data splitted into short subperiods (default 14 days), where the regression is also respectively. If more than six data points are available and when the temperature range is more than 5℃, then a reasonable regression of Reco versus temperature can be expected. At each period, the regression parameters and statistics are saved and evaluated after regressions for all periods. The three estimates of E0 with the smallest standard error are then assumed to best represent the short-term temperature response of Reco and are averaged resulting in an E0 value for the whole data set.

The third step is to, estimate of day and night time ecosystem reparation. After determing the temperature sensitivities, the respiration at reference temperature (Reco,ref) can be estimated. Because this variable is temporally changing in an ecosystem, it the Lloyd & Taylor (1994) method of Reco,ref was used to estimate the for continual 4-days periods by nonlinear regression, fixing all variables except Reco,ref.

This parameter estimated from the night time data for consecutive intervals of four days using non-linear regression of the Reco versus temperature according to above equation, where E0 is fixed to the average E0 value (for a total window size of seven days). The estimated value Reco,ref is then assigned to the central time-point of the period and linearly interpolated between periods. Subsequently, Reco can be estimated as a function of the temperature, because for each half hour the parameters E0and Reco,ref are available.

$$\mathrm{Reco(t)} = \mathrm{Rref}(t)\ e^{E0(1/(Tref-T0)-1/(T(t)-T0))}$$

……Equation 10

Fourth, using the estimates of E0 and Rref, the net ecosystem fluxes NEE (after the gap filling) are partitioned into the gross primary production GPP (gaps filled data) and ecosystem respiration Reco.

4.5. Footprint

In order to analyse the wind speed and direction influence on the turbulence, footprint was estimated as a distance in meters in the main wind direction. In this thesis, the analysis method of footprint based on Kljun et al. (2015).

4.5.1. Maximum footprint contribution

The maximum footprint contribution distance can be estimated by the peak position of the crosswind-integrated. The non-dimensional peak location derivative of equation:

$$Xmax^* = \frac{-c}{b} + d$$

……Equation 11

In this equation, Xmax* was represented maximum non-dimensional upwind distance. Based on the Nelder- Mead simplex direct search method, b equals -1.991, c equals 1.462, d equals 0.136 (Lagarias, Reeds, Wright, & Wright, 1998). So Xmax* equals 0.87.

Then, peak location x_{max} was converted from the non-dimensions to real- scale dimensions based on the equation:

$$x_{max} = 0.87\, z_m (1 - \frac{z_m}{h})^{-1} \frac{\overline{u}(z_m)}{u^*} k$$

……Equation 12

In this equation, z_m is the receptor height, h is the planetary boundary layer height, u^* is the friction velocity, $u(z_m)$ is the mean wind velocity at the measurement height, k=0.4 is the von Kármán constant.

4.5.2. Relative contribution to the total footprint area

In the application research, the interest in the fluxes is extent and location of the area. That is based on the maximum footprint contribution, the cross wind integrated footprint. It was contained the extent of the footprint at any along-wind distance from the turbulent flux tower.

From the equation:

$$X^*R = \frac{-C}{\ln(R)} + d$$

……Equation 13

And then derivation of the equation:

$$x_R = (\frac{-C}{\ln(R)} + d)\, z_m (1 - \frac{z_m}{h})^{-1} \frac{\overline{u}(z_m)}{u^*} k$$

……Equation 14

X*R is the upper limit of the footprint contain the interesting area. R is fraction of the total footprint (value between 0.1 to 0.9). The region of footprint area can be derived though the downwind (X*Rd<X*max) and upwind (X*max< X*Rd) iterative calculation. The R derived from the function of a X*R, using LPDM-B results:

$$X^*R_{d,u} = n_1 (X^*R)^{n_2} + n_3$$

……Equation 15

In the downwind limit X*Rd, n_1 equals 0.44, n_2 equals -0.77, and n_3 equals 0.24. In the upwind limit X*Ru, it contains two parts: X*max<X*Ru≤1.5, n_1 equals 0.60, n_2 equals 1.32, n_3 equals 0.61, and 1.5 <X*Ru<∞. The real- scaled distances X*Rd and X*Rd can be derived from the equation:

$$X^* = \frac{x}{z_m}(1 - \frac{z_m}{h})\frac{\overline{u}(z_m)}{u^*}k^{-1}$$

……Equation 16

4.5.3. Footprint estimates for extended time series

This footprint model is computationally inexpensive so can be easily run half-hourly time steps turbulent fluxes data. The footprint coordinate system which combined with every flux tower with its source area was performed georeferenced to geographical coordinates. In many application studies, an aggregated footprint also called footprint climatology.

5. SCENARIOS AND ANALYSIS

5.1. Quality of the eddy covariance measurements

The fluxes raw data are quality flagged by the eddyUH through the Vickers & Mahrt (1997) method. The raw data are classified according to the physical likelihood range for the high frequency values in each variable, diagnostic parameter and other tests. According to Foken et al. (2004), the classes 1 to 3 can be used for the development of parameterizations this fundamental research. Classes 4 to 6 can be used for the consecutively running system. Classes 7 to 8 can be used for the orientation. Class 9 should be excluded. Data of class NAN represents this data not a number.

Based on this method, this thesis defined the 5 classes use different colour to represent. The class 1 represented the best, and the class 9 represented the worst. Between 58 and 61% of available eddy covariance data were in 2015 and 2016, respectively. Of the three classes' fluxes, green class retained most data (42-46%), in this class the higher NEE quality data is 2015. But in this two year, both contained lot of not a number, in 2015 it partition around 38%, in 2016 it partition around 41%. Overall, generally each class data for 2015(46% for green class, 10% for orange class, 5% for yellow class, total 61% usable flux and 39% for excluded data) better than 2016(42% for green class, 11% for orange class, 5% for yellow class, total 58% usable flux and 42% for excluded data).

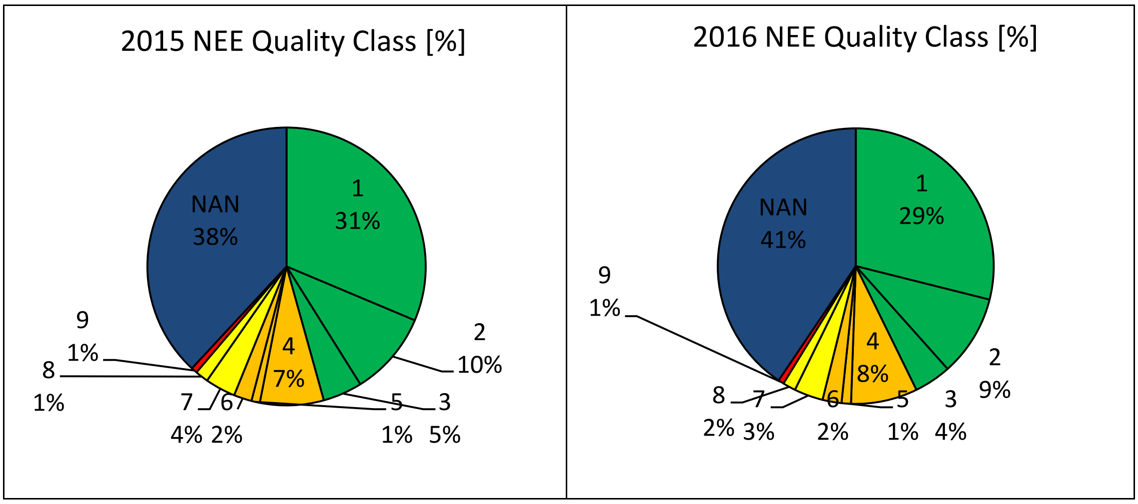

Figure 10 2015 and 2016 NEE Quality Class

Before the flux partitioning, the data have been do the gap-filled using the method of Reichstein et al.(2005). The filled data will be classified into different level (A, B, C) based on the different case (1, 2, 3). Quality flag assigned depending on gap filling method and window length: 0 represents original, 1 represents most reliable, 2 represents medium, 3 represents least reliable and 4 represents not a number. Similar to the NEE flux data, generally 2015 data is better than 2016 data. Between the 55% and 98% of flag 0 were in 2015 and 2016.In 2015, the highest proportion of flag 0 data was H, the second one is LE, NEE is the lowest one. In 2016, it presents the same trend. The more filled data in LE and NEE maybe caused by precipitation interference the open-path gas analyser system. Whereas, the flag 0 data accounted for the constant in the LE, H and NEE, due to the SND correction (described in) of H on LE. Besides, in 2015, flag 3 flux data hard appeared, but in 2016, flag 3 data occurred often. In both years flag 4 was pronounced in u* data (14% for 2015, 16% for 2016).

After applying the quality flags, NEE retained around 60% original values, of which 31% was flag 1 in 2015. NEE retained around 58% original values, of which 29% was flag 1 in 2016. It indicated that eddy covariance under a successful calculation.

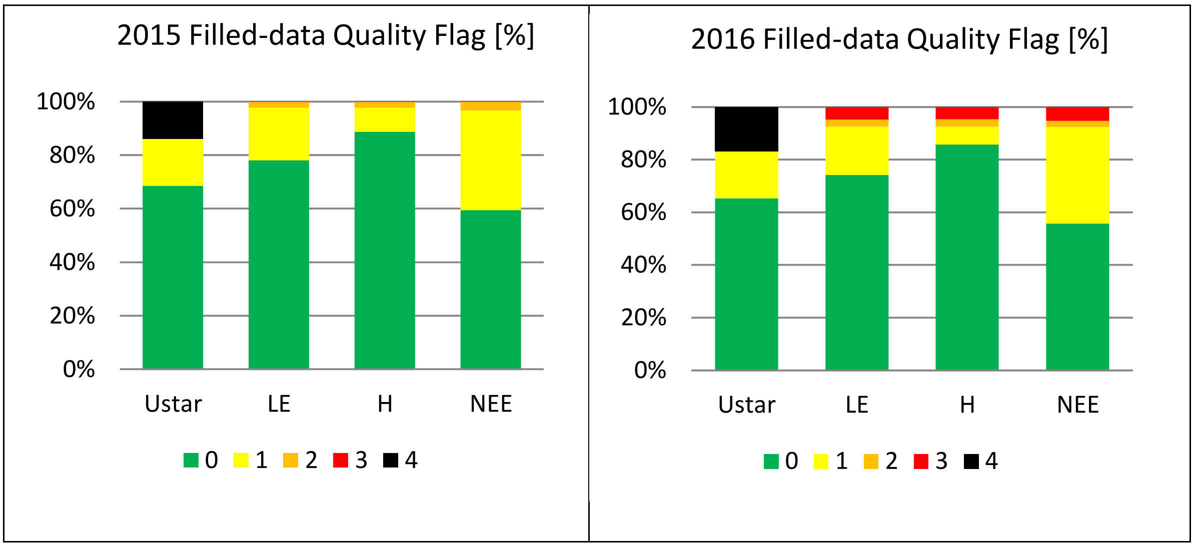

Figure 11 2015 and 2016 Filled-data Quality Flag

Figure 10 shows that, in 2015 and 2016, flag 9 data were portioned 1%, which should be excluded. Despite the high level of data used to performed data analysis more accurate, but there will be a lot of data gap. According to the eddyUH manual, a compromise approach is still using 6 to 8 class data, but this also depends on the analysis of time and the total number of operations. In this thesis, the flag 9 data were replaced by NaN, and then it will be treated as data gap. When doing gap-filling, it will be filling the data through the same meteorological condition. In 2015, 95 flag 9 data were screened out. In 2016, 954 flag 9 data were screened out.

5.2. CO_2 flux Concentration

After the fluxes had been calculated by the eddyUH, the output was be saved in monthly ascii-files. Those monthly files were aggregated and were used to estimate the cumulative sum figure in 2015 and 2016, respectively.

Because the beginning data of 2015 missing, the NEE cumulative begin at day of year (DOY) 85. As the Figure 12 shows cumulative NEE increased until DOY 265, followed by stabilization. The peak of this figure is around -1.570 g m^{-2}. From this change in trend, it obviously presented that in autumn and winter the balance of NEE budget is basically maintained.

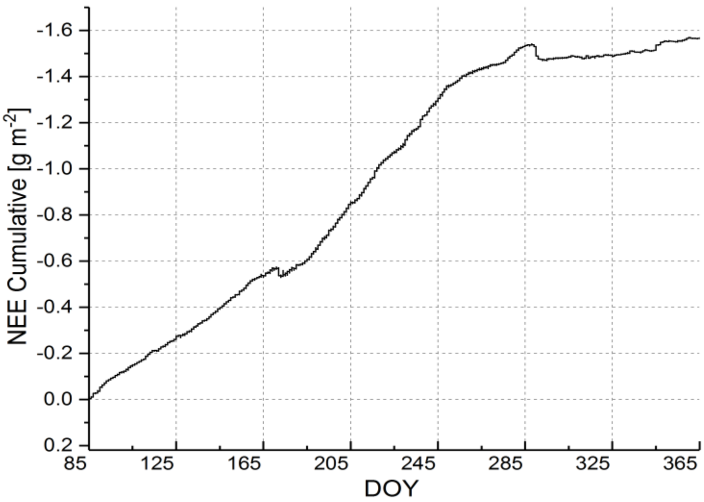

Figure 12 2015 NEE Cumulative sum

Cause the end data of 2016 are missing, the NEE cumulative end at day of year (DOY) 255. As the Figure 13 shows, cumulative NEE increased, and the overall growth trend is the same as 2015. In addition, the curve showed a smooth trend in January. This proves that the cumulative of NEE in the winter will maintain a balance. The peak of this figure is also like 2015 cumulative figure probably around the -1.6 g m^{-2}. Among them, from DOY 31 to DOY 92, the growth rate was slower. After 92 days, the slope became larger, the growth rate became faster. At the end of the curve, there has been a tendency for the slope to slow down. Thus, it can be inferred that if there is a full year of complete data, then 2016 amount of the cumulative of NEE will be the same as 2015. From this change in trend, it obviously presented that in autumn and winter the balance of NEE budget is basically maintained.

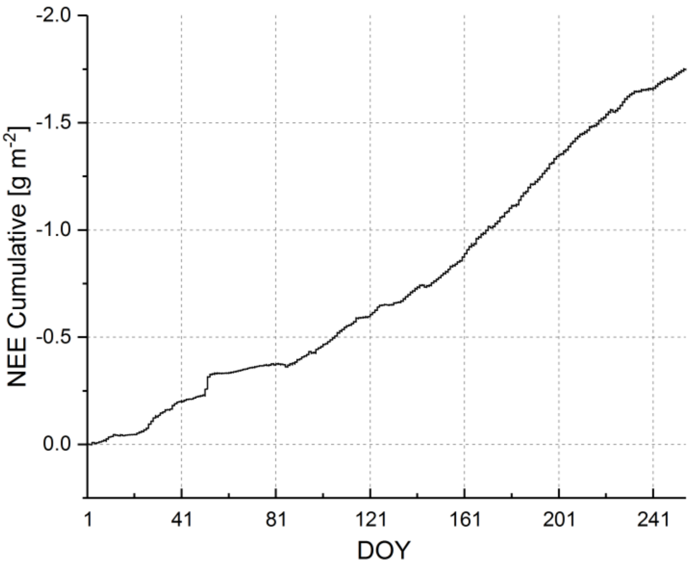

Figure 13 2016 NEE Cumulative Sum

In July 2016 as mid-summer, when NEE had the clearest diurnal cycles, it clearly saw the NEE in every day had a complete circulation, reaching a minimum every day at midday, and then gradually increased to the maximum value until midnight. In addition, it can be seen that the change of NEE was small at midnight and relatively intense at midday. This is due the fact that there is no photosynthesis at night, so no CO_2 uptake. There is only respiration. In the Figure 14, there are some spikes, which may be caused by electronic noise and physical reasons the problem.

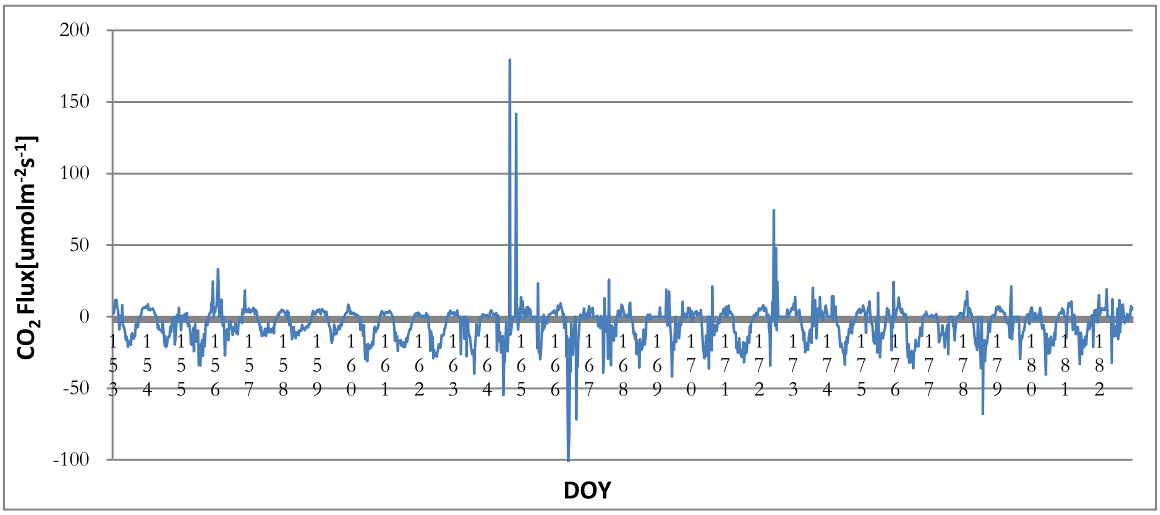

Figure 14 Half-hourly CO_2 Flux at 2016 July

A heat map is a graphical representation of data where the individual values contained in a matrix are represented as colours. In the follow heat maps, the X-axis represented the time, the Y-axis represented the month. The values of data were represented by the rainbow colour map theme. The higher the colour temperature meant the higher the value, on the contrary, the lower.

The heat maps (see Figure 16), shows spikes and noise, especially in the NEE, LE, H and GPP heat maps. As the Figure 15 shows, the amount of spikes in CO_2 flux in 2015 was more in the autumn and winter. While in 2016 was more obviously in January, February and August. The electronic noise and physical reasons may cause peak and noise such as such as inaccurate adjust the transducer of the ultrasonic anemometer, power shortage supply and electronic noise, as well as transducer water pollution, bird dropping, spider web and so on (Aubinet, Vesala, & Papale, 2012). Spike may affect all fluxes, but usually not more than 15% of the flux. While there are some conditions such as night time storage release, which look like spike, but it is natural phenomena. But spike values can usually be detected because of their amplitude, duration, or abruptness. Appropriate instruments selection, maintenance, and spike removal procedures and filtering in data processing software to help minimize the impact of such errors. In this thesis lower and upper limits were already used for raw data values and combined with Vickers & Mahrt (1997) method to reduce spike influence. Vickers & Mahrt (1997)method developed the test criteria for quality control of turbulent time series, independent of statistical distribution, with emphasis on instrument failure.

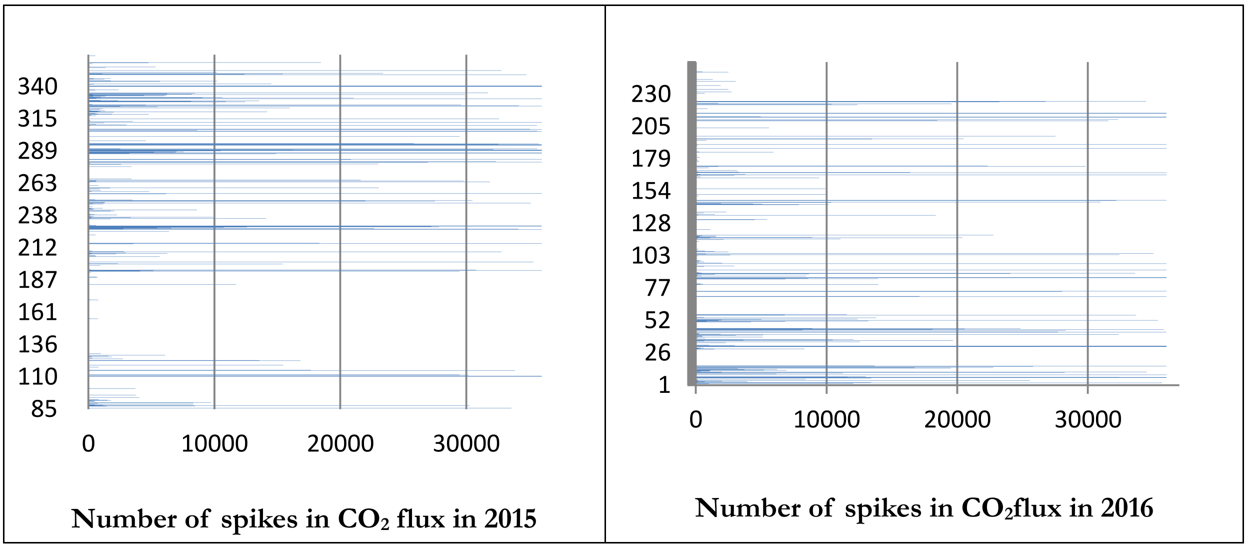

Figure 15 Number of Spikes in CO_2 Flux in 2015, 2016

As the Figure 16 shows, the biggest diurnal change in half-hourly H, LE, and NEE obviously coincided with the daytime periods. Both radiation global (Rg), sensible heat flux (H) and latent heat flux (LE) generally presente a symmetrical diurnal change, and at the peak value around midday. In contrast, the net ecosystem exchange (NEE) demonstrated a minimum value around the midday and then increasing to maximum values at the night. This trend was pronounced in the summer period. And NEE fluxes were more stable during the night than in the sunny periods during day. In addition, the NEE especially underestimated at low u* not only in short vegetation in a mountain ecosystem (Wohlfahrt et al., 2008), but also grasslands (Gilmanov et al., 2007) and forests (Papale et al., 2006) which is falter and less complex terrain. So, the night-time turbulent fluxes energy change was smaller than daytime fluxes. The change of NEE fluxes coincided with the air temperature (Ta) more or less, the high NEE occur with the warmer temperature. But this is also due to the correlation between irradiance and temperature. NEE first follows radiation, temperature is the next important factor (and day of the year). The day time CO_2 reduction in the high air temperature maybe have two causes: under the high Ta closured stomatal could inhibited plant photosynthesis, the deficits of soil water led to the lower potentials of leaf water (Damour, Simonneau, Cochard, & Urban, 2010) and increased Ta with the forest respiration (Lloyd & Taylor, 1994). However, the values of LE and H in the consecutive middays presented an inverse relationship: high relative humidity (rh) company with the high H and low LE. This trend also appeared in the relationship between LE, H and air temperature (Ta). At the midday high LE was observed with the high Ta, while the E was observed low, particularly in 2016.

In basic principle, the net ecosystem fluxes are partitioned into the gross primary production and ecosystem respiration. So as the Figure 16 shown, the half-hourly NEE, Reco and GPP also show a large diurnal change between the daytime periods. In the Reco heat maps, the value changed with the sunny periods. Values of GPP got peak at the midday then gradually decreased the lowest value at the night. This was due to plant photosynthesis, and in summer the photosynthesis of plants was greater. However, under the hot climate, plants in order to avoid excessive evaporation of water will close the stomata. So in some very high air temperature midday, plant respiration does not increase but will reduce.

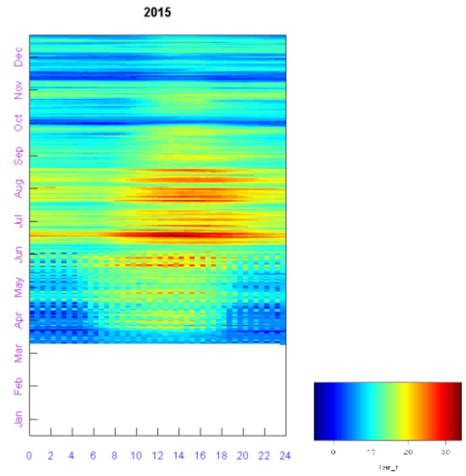

2015 Air Temperature [℃]

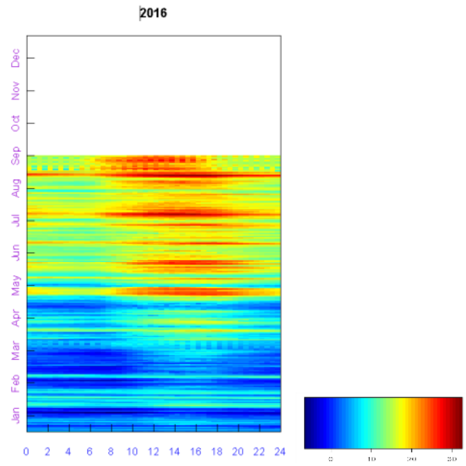

2016 Air Temperature [℃]

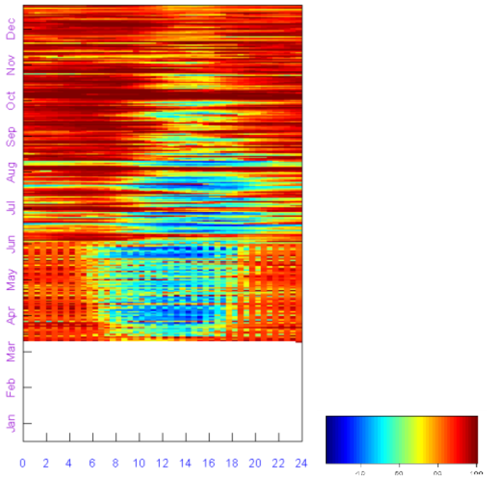

2015 Relative Humidity [%]

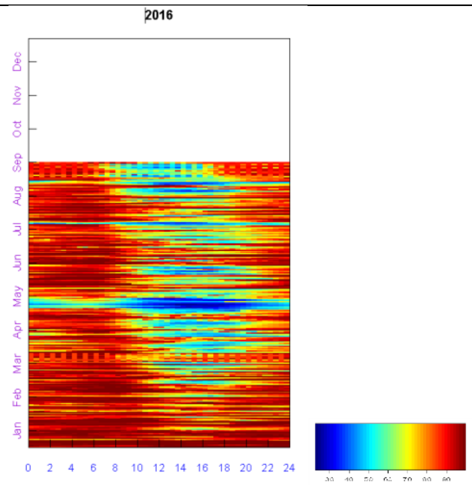

2016 Relative Humidity [%]

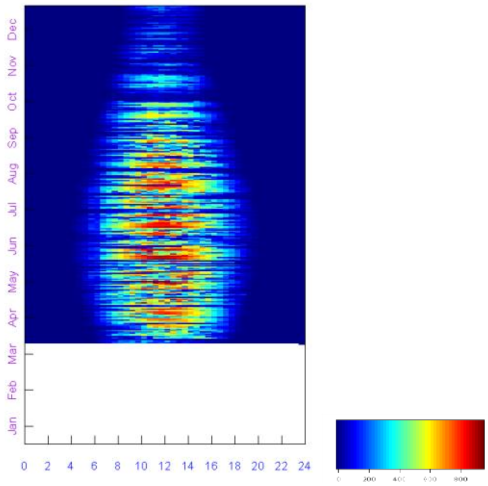

2015 Radiation Global [Wm^{-2}]

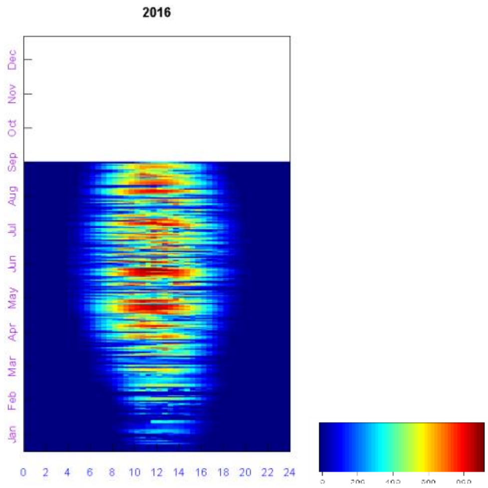

2016 Radiation Global [Wm^{-2}]

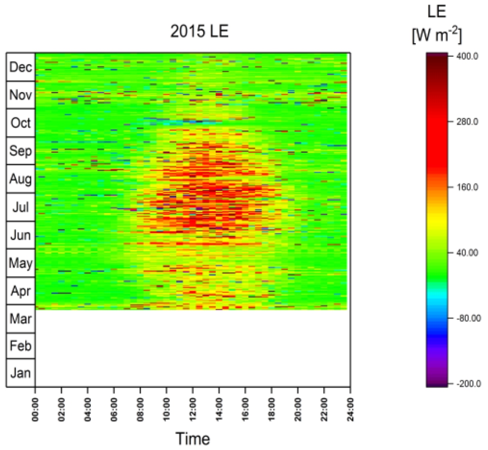

2015 Latent Heat Flux [Wm-2]

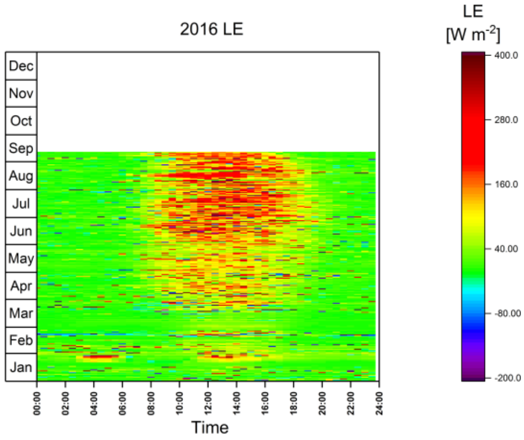

2016 Latent Heat Flux [Wm-2]

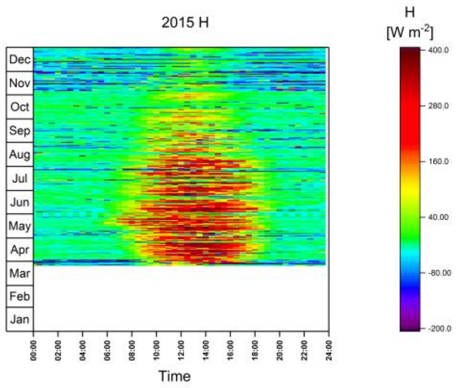

2015 Sensible Heat Flux [Wm-2]

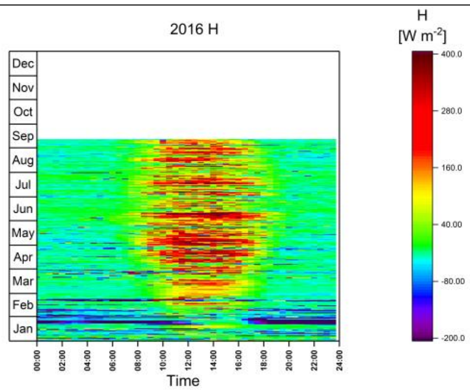

2016 Sensible Heat Flux [Wm-2]

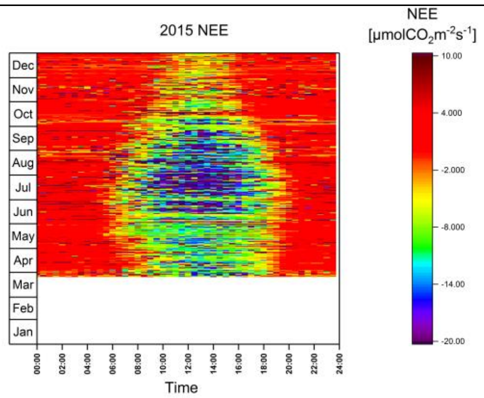

2015 Net Ecosystem Exchange [umolCO2m-2s-1]

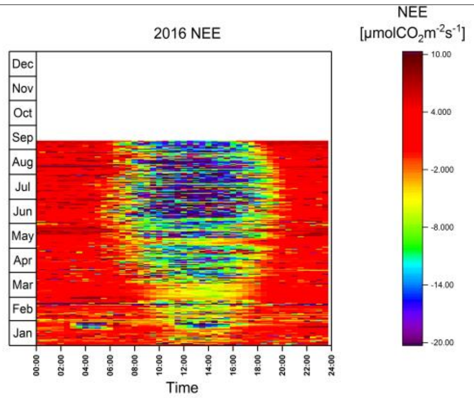

2016 Net Ecosystem Exchange [umolCO2m-2s-1]

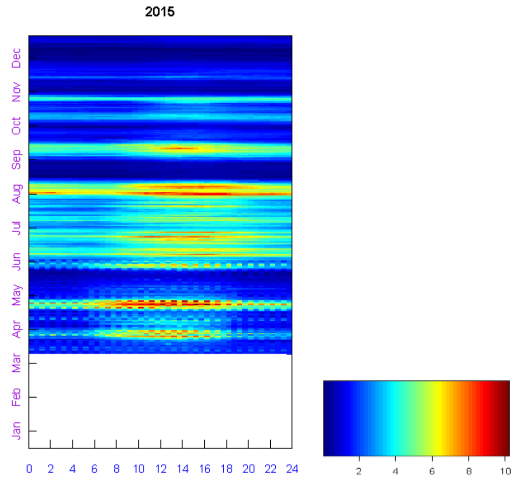

2015 Respiration Ecosystem
[umol$CO_2m^{-2}s^{-1}$]

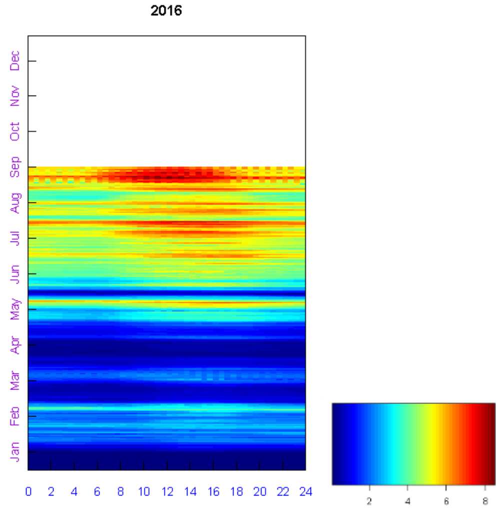

2016 Respiration Ecosystem
[umol$CO_2m^{-2}s^{-1}$]

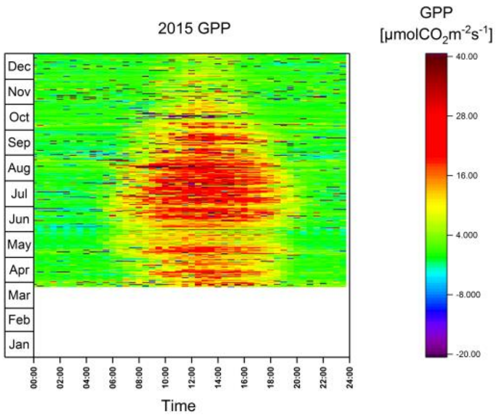

2015 Gross Primary Productivity
[umol $CO_2m^{-2}s^{-1}$]

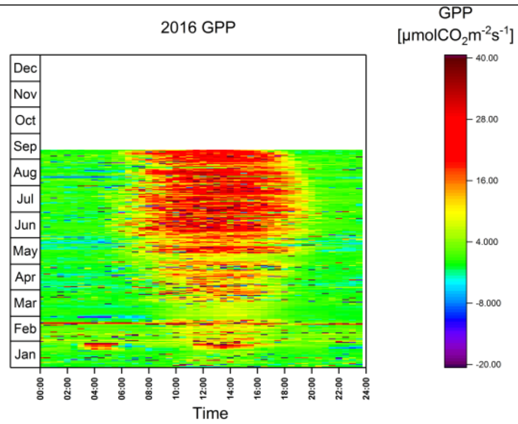

2016 Gross Primary Productivity
[umol$CO_2m^{-2}s^{-1}$]

Figure 16 Heat Maps Illustrating Weather and Flux Dynamics in 2015, 2016

As shown in Figure 17, the diurnal cycle of half-hourly NEE values were exhibited an obvious V-shape. A negative value for NEE occurred daytime (between 6 a.m. to 19 p.m.), indicated that the forest appeared as a sink of CO_2 during the daytime. While in the evening, showing positive, it was as a source of CO_2. NEE reached the minimum value around -13 μ mol m^{-2} s^{-1}at noon. GPP presented a completely opposite trend to NEE, at noon reached the highest point, and then slowly reduced until midnight. This is related to plant photosynthesis during the day. Reco was always maintained in a steady state, because the plants are always respiration.

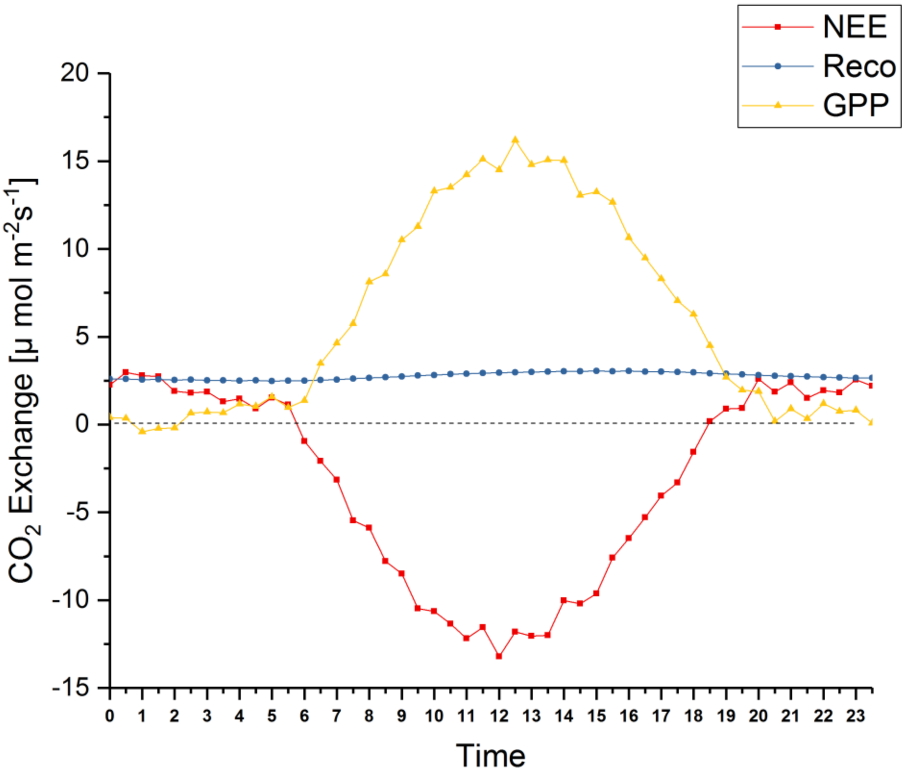

Figure 17 2016 Diurnal Cycle in NEE, GPP, Reco

Figure 18 GPP Diurnal Cycle in Original Data, Quality Control Data and in Different YearFigure 18 compares the raw data values for 2015 and 2016 diurnal cycle GPP and after the quality control values. It can be seen, 2015 and 2016 the overall diurnal cycle GPP difference is not very large, the maximum value is about 16 μ mol m^{-2} s^{-1}. Before and after quality control eliminates the influence of some outliers. For data performance have a certain positive effect. However, this does not remove the outliers completely, as will be seen in Figure 19 and Figure 20 below.

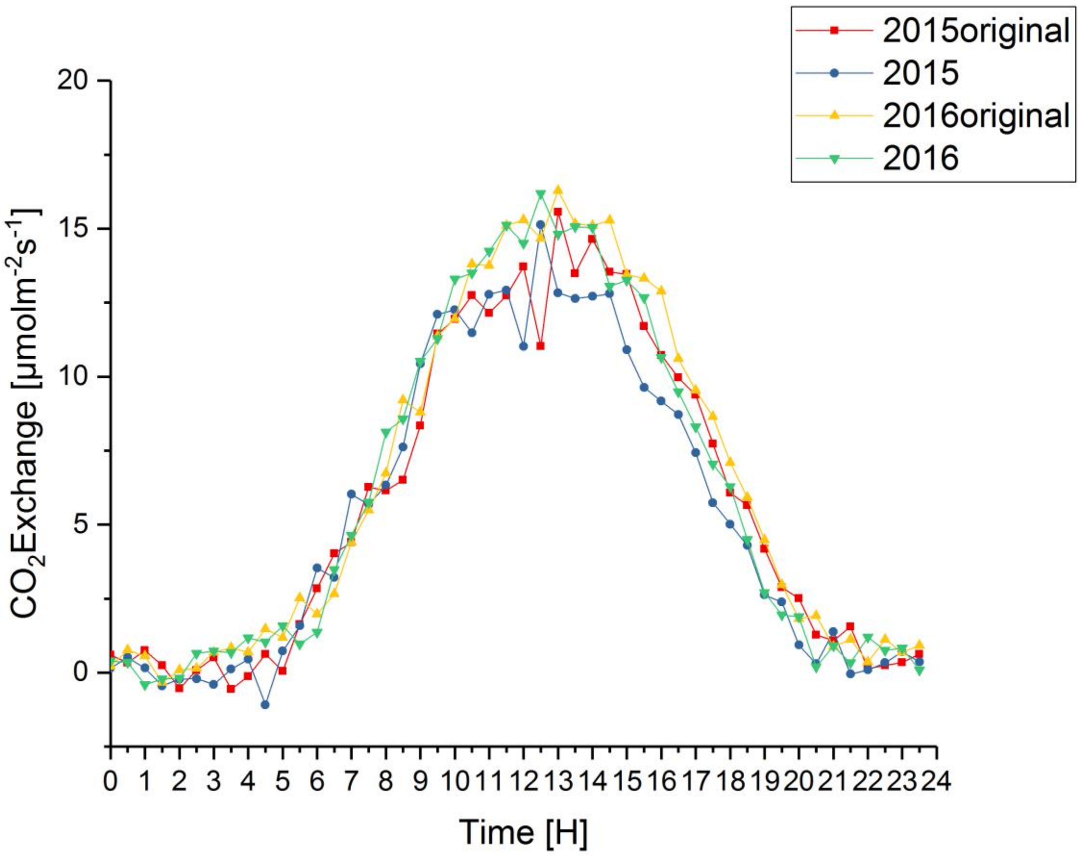

Figure 18 GPP Diurnal Cycle in Original Data, Quality Control Data and in Different Year

GPP denotes the CO_2 uptake due to photosynthesis. The daily GPP are shown in Figure 19 and Figure 20in 2015 and 2016. During the plants non-growing season, the GPP was close to zero. When the growing season begin the GPP was gradually increased until to summer arrived the maximum value (on day of the year 230 in 2015, on day of the year 166 in 2016). In the autumn, the GPP began to decreased, because the plant leaves withered and the air temperature decreased. In 2015, the cumulative NEE was -1.57 CO_2 g m^{-2}, and the cumulative GPP was 3.13 CO_2 g m^{-2}. In 2016, the cumulative NEE was -1.75 CO_2 g m^{-2}, and the cumulative GPP was 3.23 CO_2 g m^{-2}. This two year value was not much difference. 2016 was slightly larger than 2015.

As the shown in Figure 19, very significant outliers appear which not matched the trend of the daily GPP curve. In 2015, at DOY 172 the outlier was -22.65 g m^{-2} d^{-1}, at DOY 209 the outlier was -65.06 g m^{-2} d^{-1} and DOY 347 the outlier was 42.88 g m^{-2} d^{-1}. In 2016, at DOY 51 the outlier was 54.80 g m^{-2} d^{-1}, at 52 the outlier was 112.65 g m^{-2} d^{-1}, and DOY 85 and DOY 96 were performed negative anomalies. Although in this thesis already done the quality control, these values were still not match with the trend curve. Therefore, in order to eliminate the influence of these abnormal values, this study selected 95% confidence interval according to the normal distribution of the data, and according to the reality situation and the trend of the curve, eliminated the outliers in 2015 and 2016. Then according to the curve change rule, the data gapes were linearly interpolated, and the GPP of 2015 and 2016 were obtained as shown in Figure 20 . The average daily GPP for 2015 is 20.15 g m^{-2} d^{-1}, 2016 is 22.38 g m^{-2} d^{-1}.

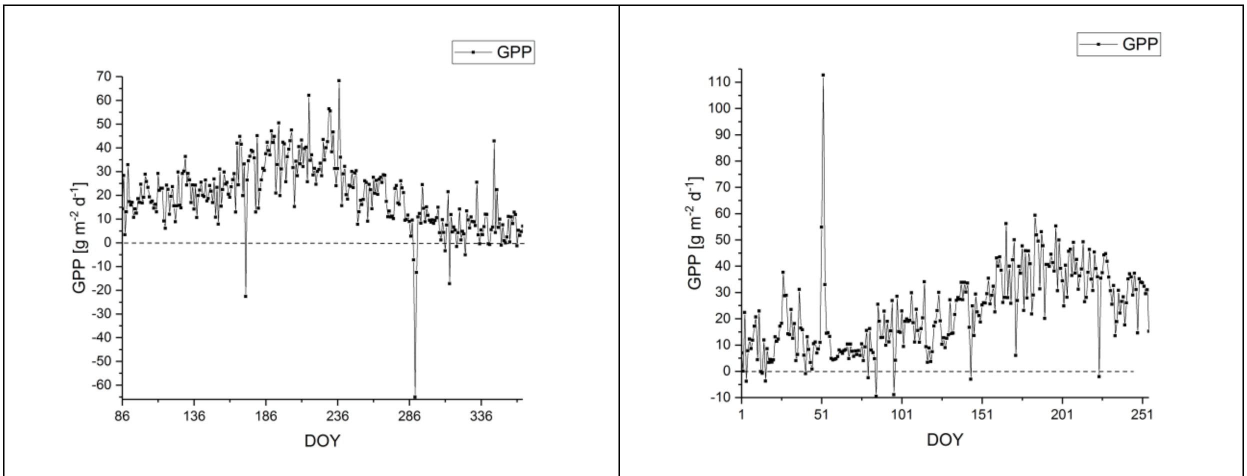

2015 Daily Values of GPP

2016 Daily Values of GPP

Figure 19 Daily Values of GPP in 2015 and 2016

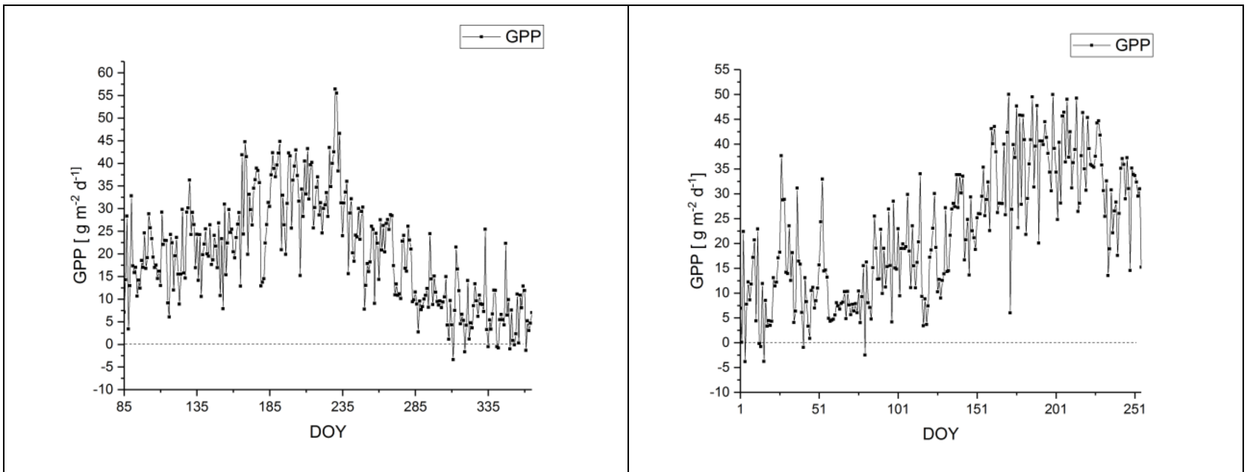

2015 Daily Values of GPP after Filtrate

2016 Daily Values of GPP after Filtrate

Figure 20 Daily Values of GPP after Filtrate in 2015 and 2016

5.3. Footprint under Different wind speed and direction

From the wind rose (Figure 21), it can obviously presented that the major wind direction was around south west, and the major wind speed was between 2 to 6 m s^{-1} in 2015 whole year. The footprint map was also consistent with the wind rose map shown. The major direction is south west. The wind speed was largest in the south southwest direction.

A basic characteristic of the footprint principal is that, the most of the turbulent contribution does not come from underneath the tower and not from many far form away, but rather from somewhere in the between. The higher the measurement height, the greater area underneath the flux tower a zero contribution. As the Figure 22 shows, the flux tower below the flux tower was almost zero. This situation also appeared at far from the tower. Between those two areas, the footprint gradually increased.

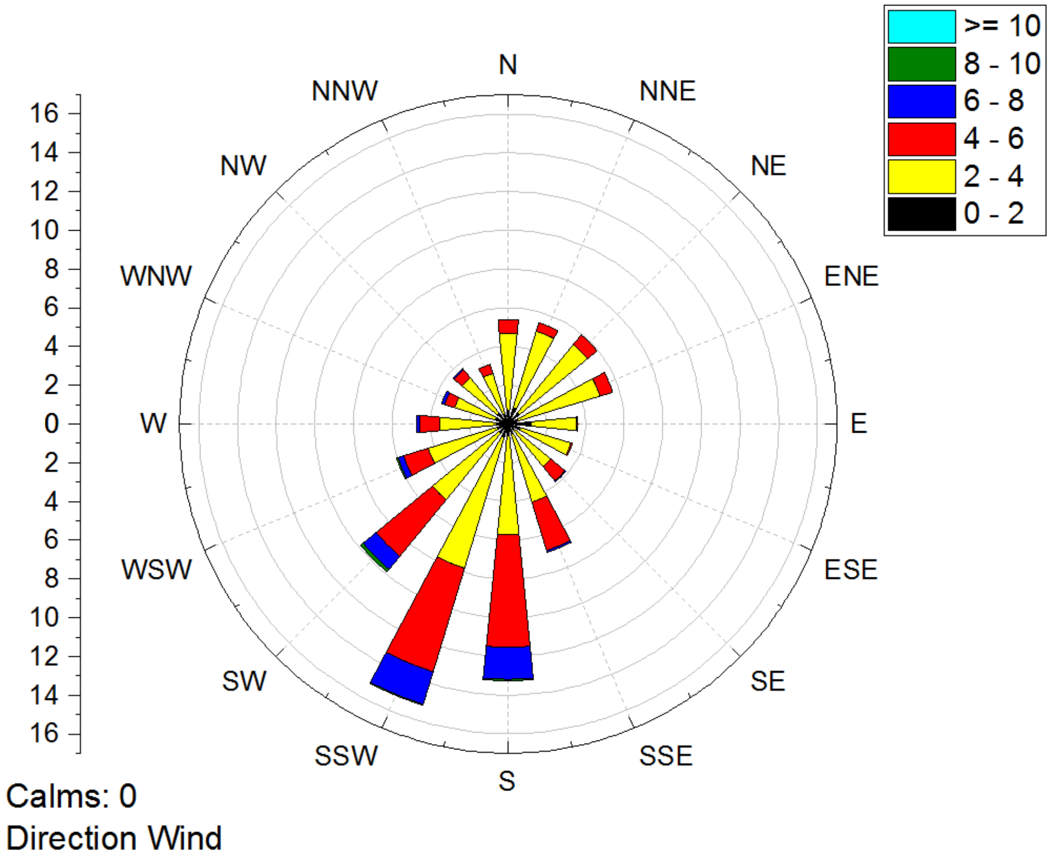

Figure 21 2015 Wind Rose

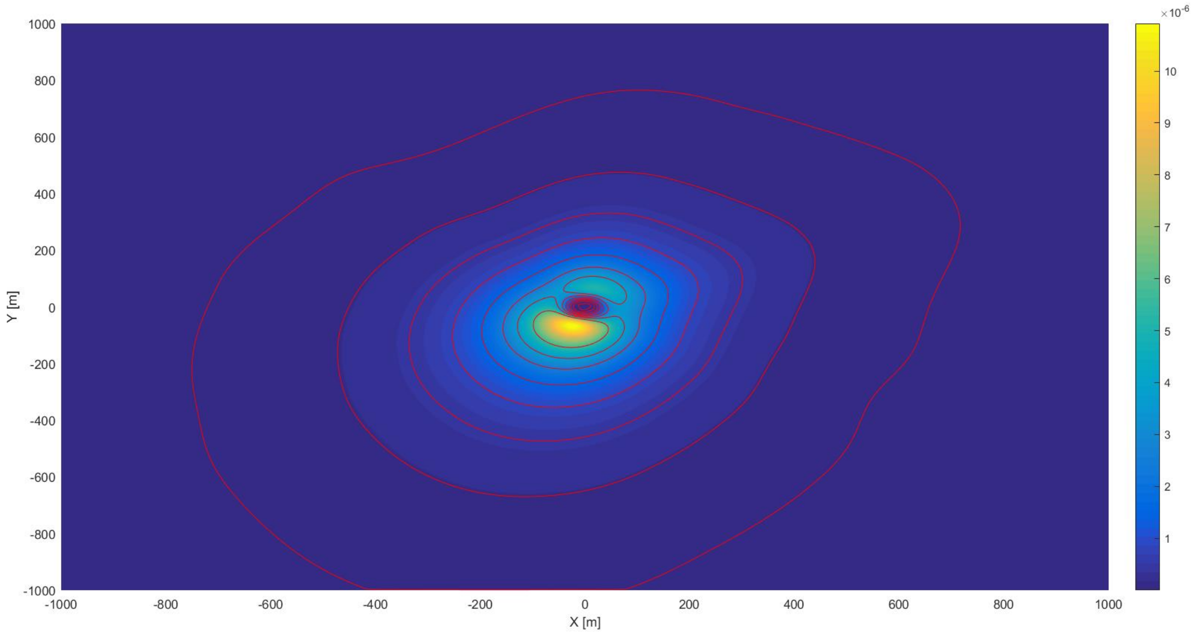

Figure 22 2015 Footprint climatology

From the Figure 23 wind rose, it can obviously presented that in 2016, the trend of the major wind direction was the same as in 2015, notably south west, and the major wind speed was also similar to 2015. The footprint map was also consistent with the wind rose map shown. The major direction is south west. The wind speed largest in the south southwest direction, so in the footprint map the in the direction of south southwest also have the largest influence. Since the height of the measurement has a great impact on the footprint, while the height of the measuring tower is fixed, so the size of footprint in different years, 2015 and 2016 had shown the same arrange(the major of flux came from an upwind distance from 20m to 800m). But, on the part of the maximum value which in 2015 slightly larger than in 2016.

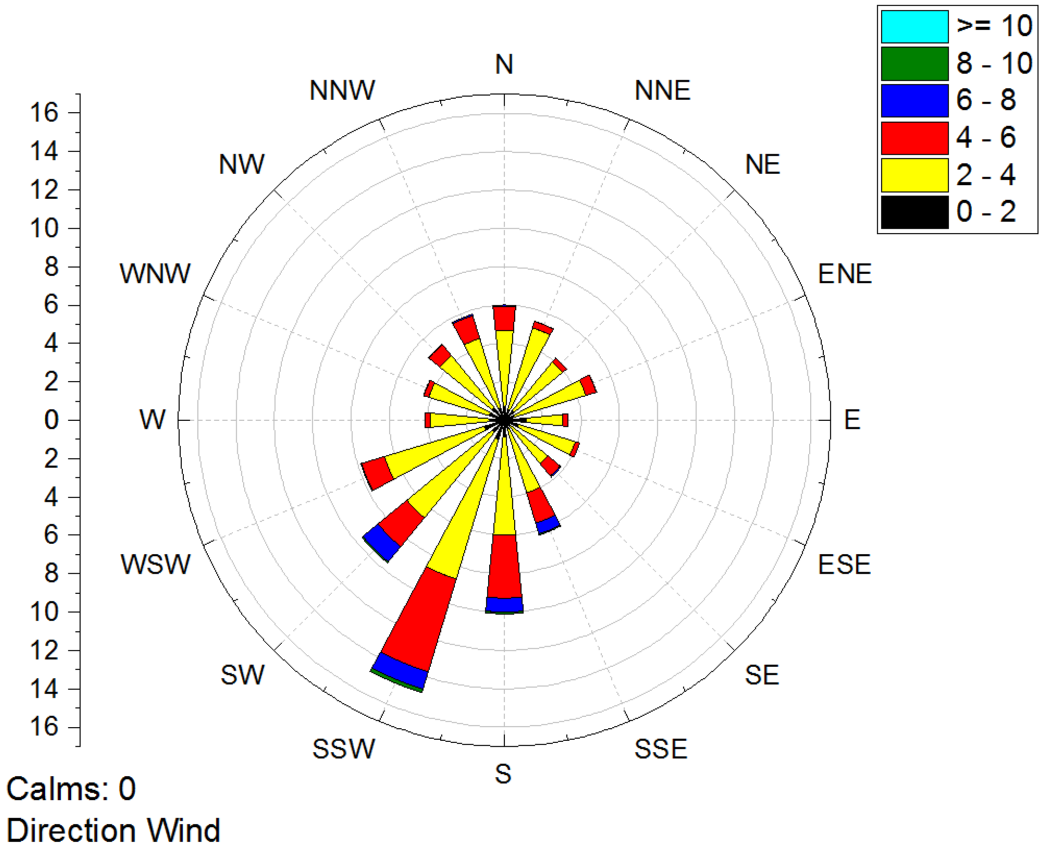

Figure 23 2016 Wind Rose

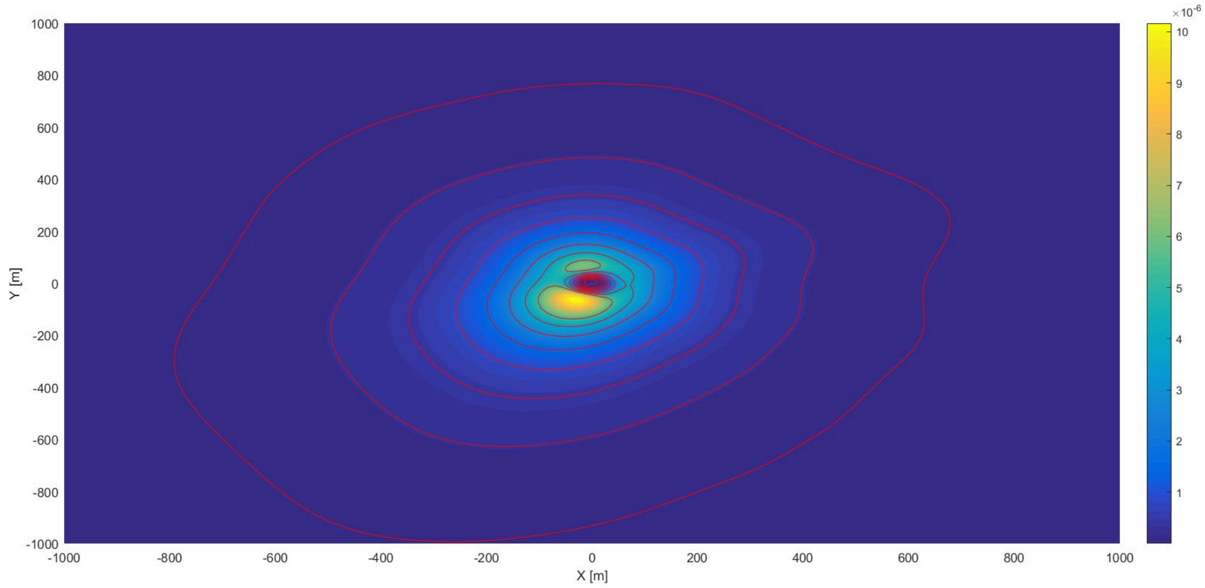

Figure 24 2016 Footprint Climatology

Figure 25 shows the footprint areas for the flux tower, overlay on a study area remote image in 2016. It can clearly found which range of footprint was affected by the Douglas fir. Douglas fir on the image presented a special texture which cans easily vectorization in Arcgis. Douglas fir presented a trapezoidal shape. Overlay the after georeferenced footprint map on the image and did the map calculation. Based on the simply calculate, 9.26 % of the footprint was in the Douglas fir. Due to this two year the turbulent flux tower in the same position, underlying surface roughness was no change and there were no significant fluctuation in the meteorology and thermal condition. So in two years the footprint climatology there is no significant change. As mentioned by Vesala et al.(2006) said, the prediction of the forest footprint is mainly determined by two factors: canopy turbulence and the source/sink levels within the canopy. These factors for close observation of the treetops level become of particular relevant.

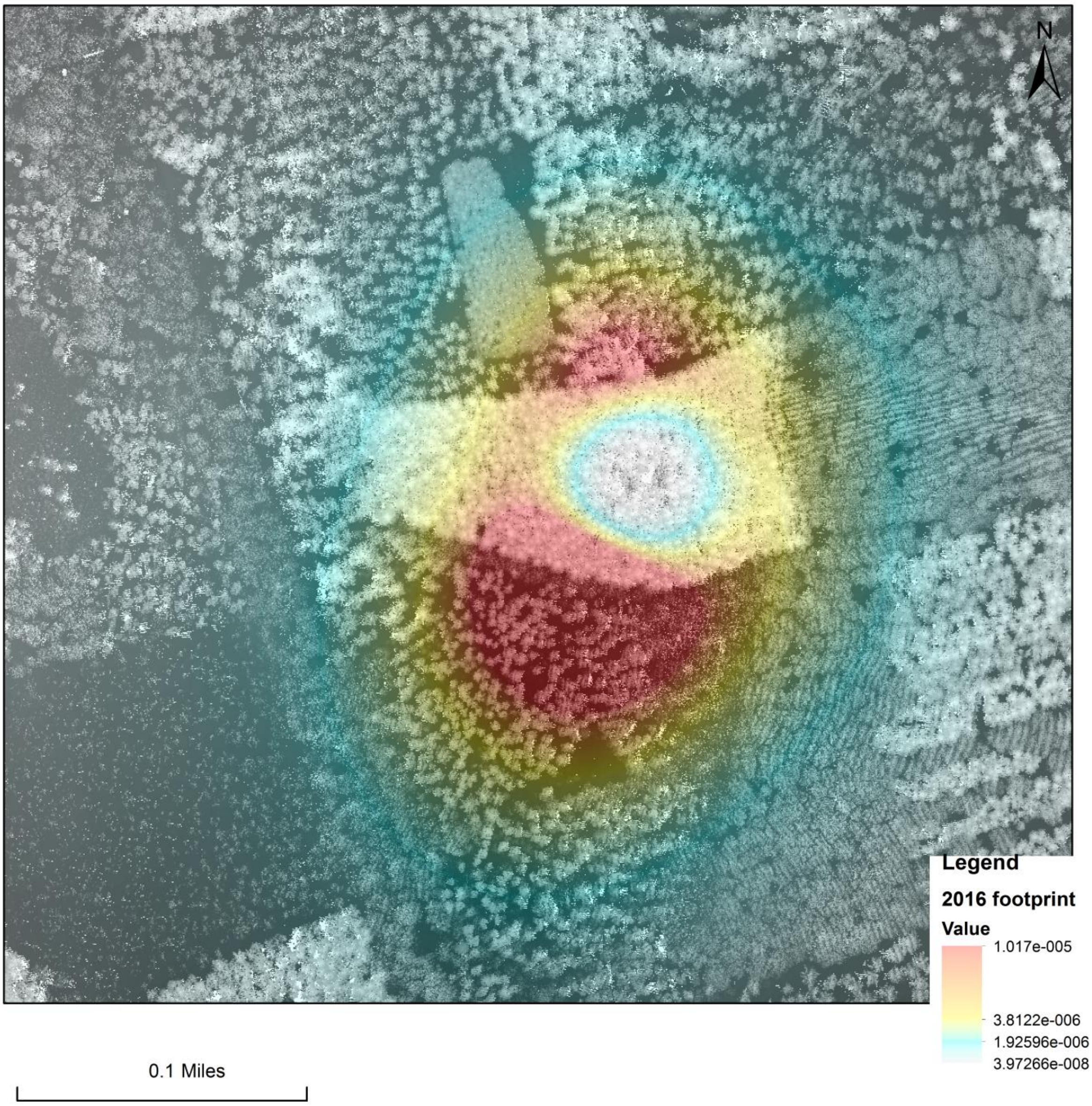

Figure 25 Footprint Climatology Overlay with Image in 2016

Error! Reference source not found. shows DOY 15(Jan, in winter) and DOY 198(Jul, in summer) midnight and noon footprints and cumulative footprint contours. The footprint contours were shown in steps of 10% from 10% to 80%. From the midnight and the noon on the two map comparison, it was clear that the footprint affected area at midnight was larger than the noon, showed an oval shape. At noon showed a narrow shape. This is the case both occurred in DOY 15 and DOY 198. In contrast to the different seasons, the summer footprint affected area both at noon and at midnight is not as large as winter.

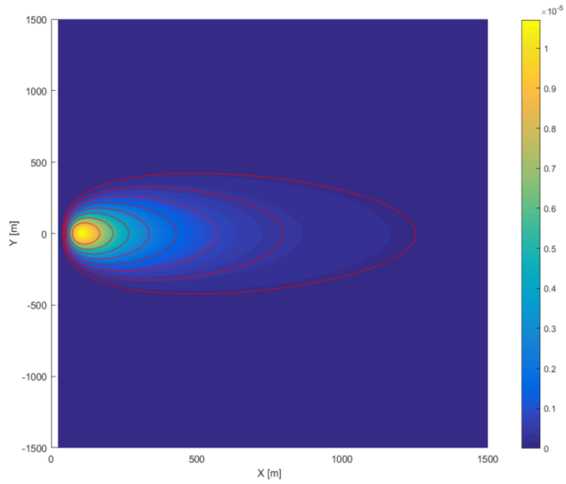

DOY 15 Midnight Footprint

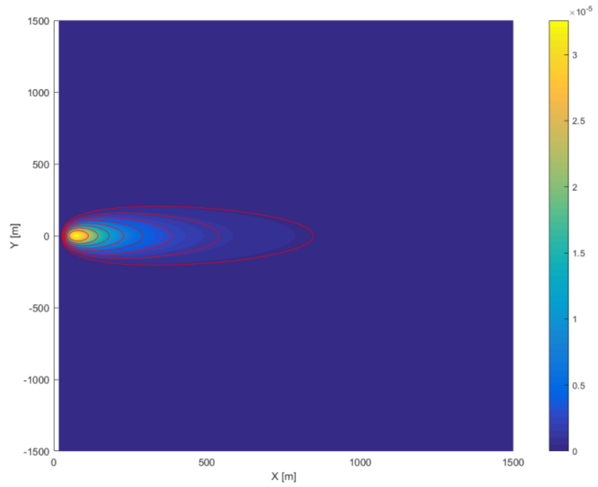

DOY 15 Noon Footprint

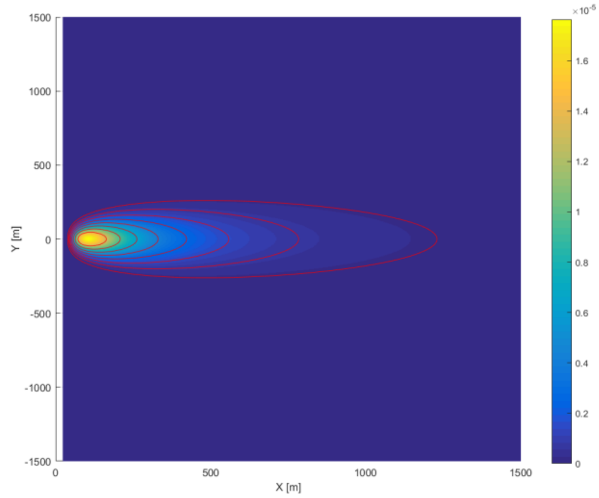

DOY 198 Midnight Footprint

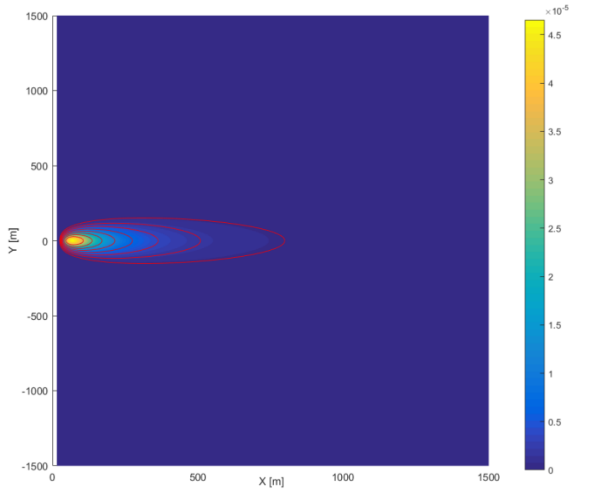

DOY 198 Noon Footprint

Figure 26 Footprint Maps in Different Daytime

6. CONCLUSIONS AND RECOMMENDATIONS

6.1. Conclusions

In this study, we obtained the raw Eddy Covariance of Speulderbos and pre-processed the raw data with eddyUH. Based on the Vickers & Mahrt (1997) method to filter the raw data, the good data (flags 1 to 8) accounted of 61% and 58%, in 2015 and 2016 respectively. Flag 9 data, the poorest quality, accounted for 1% of the total data. The NAN data accounted for 38% and 41%, in 2015 and 2016 respectively. Through the eddyUH calculate the cumulative of NEE is -1.567 g m^{-2} and the peak is -1.570 g m^{-2} in 2015. Cumulative of NEE is -1.747 g m^{-2} and the peak is -1.752 g m^{-2} in 2016.
In the quality control, the overall diurnal cycle GPP difference is not very large, the maximum value is about 16 μ mol m^{-2} s^{-1}. Before and after quality control eliminates the influence of some outliers.
Before the flux partitioning, the data will be classified into different level. In 2015, NAN of Ustar accounted for 14%. The best data quality performance is H. In 2016, NAN of Ustar accounted for 16%. The best data quality performance is H, but in H, LE and NEE all of appearance the flag 3.Then use the consecutive data under the Reichstein et al. (2005) method to do the flux partitioning, the GPP and Reco were obtained. The average daily GPP for 2015 is 20.15 g m^{-2} d^{-1}, 2016 is 22.38 g m^{-2} d^{-1}.
And we analysed the relationship between the air temperature, relative humidity, NEE, H, LE, Reco and GPP. H, LE, and NEE obviously coincided with the daytime periods, H and LE at the peak value around midday, while NEE had a contrast situation. Reco and GPP also show a large diurnal change. The GPP got peak at the midday, same as Reco.
In the footprint, we use the Kljun et al.(2015) method and combined with the wind speed and direction to obtain the footprint climatology. Overlay the remote image, got the 9.26 % of the footprint was in the Douglas fir.

6.2. Recommendations

For the turbulent fluxes pre-processing software, the eddy covariance flux estimated strongly affected by the data selection, project of processing steps and the correct application. New methods and theories always arise early in the software development. In the future study, do not use eddyUH because there are better seawares such as eddyPro, it can provide latest correction methods, supply the latest eddy covariance measurement instruments, easily deal with more flexible data format and export the more exquisite pictures.
For the data selection, because the turbulent flux have the spike and easily affected by the instruments and outside surrounding. So the proper data selected method is necessary. As the Foken et al. (2004) method said, use only flags 1 to 3 for fundamental research and flags 4 to 6 for continuously running systems.
Flux tower data include also other species than Douglas fir, therefore the eddy covariance data should be compared to LAI data of different species such as Scotch pine and beech.
As far as the verification of turbulent fluxes, it has a close connection with the energy balance. Whether the turbulent fluxes are in line with energy balance should be looked further into.

LIST OF REFERENCES

Arrhenius, S. (1889). Über die Reaktionsgeschwindigkeit bei der Inversion von Rohrzucker durch Säuren. *Zeitschrift Für Physikalische Chemie*, *4*, 226–248.

Asante-yeboah, E. (2010). Assessing the impacts of Silvicultural treatment systems on Ecosystem services : a case of Carbon sequestration and Biodiversity conservation. *Geo-Information Science*, 82.

Aubinet, M., Vesala, T., & Papale, D. (2012). *Eddy Covariance: A Practical Guide to Measurement and Data Analysis*. http://doi.org/10.1007/978-94-007-2351-1

Bonan, G. B. (2008). Forests and climate change: forcings, feedbacks, and the climate benefits of forests. *Science*, *320*(5882), 1444–1449. http://doi.org/10.1126/science.1155121

Burba, G. (2013). Eddy Covariance Method.

Damour, G., Simonneau, T., Cochard, H., & Urban, L. (2010). An overview of models of stomatal conductance at the leaf level. *Plant, Cell and Environment*, *33*(9), 1419–1438. http://doi.org/10.1111/j.1365-3040.2010.02181.x

Evans, J. G., McNeil, D. D., Finch, J. W., Murray, T., Harding, R. J., Ward, H. C., & Verhoef, A. (2012). Determination of turbulent heat fluxes using a large aperture scintillometer over undulating mixed agricultural terrain. *Agricultural and Forest Meteorology*. http://doi.org/10.1016/j.agrformet.2012.07.010

Falge, E., Baldocchi, D., Olson, R., Anthoni, P., Aubinet, M., Bernhofer, C., … Wofsy, S. (2001). Short communication: Gap filling strategies for long term energy flux data sets. *Agricultural and Forest Meteorology*, *107*(1), 71–77. http://doi.org/10.1016/S0168-1923(00)00235-5

Falge, Baldocchi, Olson, Anthoni, & Aubinet. (2001). Gap filling stratergies for defansible annual sums of net ecosystem exchange. *Papers in Natural Reasources*.

Fang, J. Y., Chen, A., Peng, C., Zhao, S., & Ci, L. (2001). Changes in forest biomass carbon storage in China between 1949 and 1998. *Science*. http://doi.org/10.1126/science.1058629

Field, C. B., Raupach, M. R., & Victoria, R. (2003). The global carbon cycle: Integrating humans, climate and the natural world. *The Global Carbon Cycle: Integrating Humans, Climate and the Natural World*.

Finkelstein, P. L., & Sims, P. F. (2001). Sampling error in eddy correlation flux measurements. *Journal of Geophysical Research*. http://doi.org/10.1029/2000JD900731

Foken, T., Gockede, M., Mauder, M., Mahrt, L., Amiro, B., & Munger, W. (2004). {P}ost-field data quality control. *{H}andbook of {M}icrometeorology*, *29*(1988), 181–208. http://doi.org/10.1007/1-4020-2265-4_9

Gilmanov, T. G., Soussana, J. F., Aires, L., Allard, V., Ammann, C., Balzarolo, M., … Wohlfahrt, G. (2007). Partitioning European grassland net ecosystem CO2 exchange into gross primary productivity and ecosystem respiration using light response function analysis. *Agriculture, Ecosystems & Environment*, *121*(1), 93–120. http://doi.org/10.1016/j.agee.2006.12.008

Hojstrup, J. (1993). A statistical data screening procedure. *Measurement Science and Technology*. http://doi.org/10.1088/0957-0233/4/2/003

HORST, T. W. (1997). A SIMPLE FORMULA FOR ATTENUATION OF EDDY FLUXES MEASURED WITH FIRST-ORDER-RESPONSE SCALAR SENSORS. *Boundary-Layer Meteorology*, *82*(2), 219–233. http://doi.org/10.1023/A:1000229130034

Houghton JT, Ding, Y., Griggs, D., Noguer, M., van der Linden, P., Dai, X., … Johnson, C. (2001). Climate Change 2001: The Scientific Basis. *Climate Change 2001: The Scientific Basis*, 881. http://doi.org/10.1256/004316502320517344

Ipcc Wg1. (2003). IPCC meeting on current scientific understanding of the processes affecting terrestrial carbon stocks and human influences upon them, (July), 1–37.

Jaeger, L., & Kessler, A. (1997). Twenty years of heat and water balance climatology at the Hartheim pine forest, Germany. *Agricultural and Forest Meteorology*. http://doi.org/10.1016/S0168-1923(96)02372-6

Jiyuan, L., & Guirui, Y. (2010). A method of geo-information science for studying carbon cycle and its mechanism of terrestrial ecosystems. *Geo Graphical Research*, *22*(4), 397–405.

Kljun, N., Calanca, P., Rotach, M. W., & Schmid, H. P. (2003). a Simple Parameterisation for Flux Footprint Predictions, 503–523.

Kljun, N., Calanca, P., Rotach, M. W., & Schmid, H. P. (2015). A simple two-dimensional parameterisation for Flux Footprint Prediction (FFP). *Geoscientific Model Development*, *8*(11), 3695–3713. http://doi.org/10.5194/gmd-8-3695-2015

Kramer, P. J. (1981). Carbon dioxide concentration, photosynthesis, and dry matter production. *BioScience*. Retrieved from http://www.jstor.org/stable/1308175

Lagarias, J. C., Reeds, J. A., Wright, M. H., & Wright, P. E. (1998). Convergence Properties of the Nelder--Mead Simplex Method in Low Dimensions. *SIAM Journal on Optimization*, *9*(1), 112–147. http://doi.org/10.1137/S1052623496303470

Lee, X., & Massman, W. J. (2011). A Perspective on Thirty Years of the Webb, Pearman and Leuning Density Corrections. *Boundary-Layer Meteorology*, *139*(1), 37–59. http://doi.org/10.1007/s10546-010-9575-z

Lloyd, J., & Taylor, J. A. (1994). On the temperature dependence of soil respiration. *Functional Ecology*, *8*(3), 315–323. http://doi.org/papers2://publication/uuid/EE45B025-598C-4D7C-A259-FA6366F27CAB

Lovett, G. M., Cole, J. J., & Pace, M. L. (2006). Is net ecosystem production equal to ecosystem carbon accumulation? *Ecosystems*, *9*(1), 152–155. http://doi.org/10.1007/s10021-005-0036-3

Mammarella, I., Peltola, O., Nordbo, A., Järvi, L., & Rannik, Ü. (2016). EddyUH: an advanced software package for eddy covariance flux calculation for a wide range of instrumentation and ecosystems. *Atmospheric Measurement Techniques Discussions*, (January), 1–33. http://doi.org/10.5194/amt-2015-323

Papale, D., Reichstein, M., Aubinet, M., Canfora, E., Bernhofer, C., Kutsch, W., … Yakir, D. (2006). Towards a standardized processing of Net Ecosystem Exchange measured with eddy covariance technique: algorithms and uncertainty estimation. *Biogeosciences*, *3*(4), 571–583. http://doi.org/10.5194/bg-3-571-2006

Peltola, O., Mammarella, I., Haapanala, S., Burba, G., & Vesala, T. (2013). Field intercomparison of four methane gas analyzers suitable for eddy covariance flux measurements. *Biogeosciences*, *10*(6), 3749–3765. http://doi.org/10.5194/bg-10-3749-2013

Raj, R., Hamm, N. A. S., van der Tol, C., & Stein, A. (2014). Variance-based sensitivity analysis of BIOME-BGC for gross and net primary production. *Ecological Modelling*, *292*, 26–36. http://doi.org/10.1016/j.ecolmodel.2014.08.012

Rannik, Ü., & Vesala, T. (1999). Autoregressive filtering versus linear detrending in estimation of fluxes by the eddy covariance method. *Boundary-Layer Meteorology*, *91*(2), 259–280. http://doi.org/10.1023/A:1001840416858

Reichstein, M., Falge, E., Baldocchi, D., Papale, D., Aubinet, M., Berbigier, P., … Valentini, R. (2005). On the separation of net ecosystem exchange into assimilation and ecosystem respiration: Review and improved algorithm. *Global Change Biology*, *11*(9), 1424–1439. http://doi.org/10.1111/j.1365-2486.2005.001002.x

Schimel, D. S., House, J. I., Hibbard, K. a, Bousquet, P., Ciais, P., Peylin, P., … Wirth, C. (2001). Recent patterns and mechanisms of carbon exchange by terrestrial ecosystems. *Nature*, *414*(6860), 169–172. http://doi.org/10.1038/35102500

Schmid, H. P. (1994). Source areas for scalars and scalar fluxes. *Boundary-Layer Meteorology*, *67*(3), 293–318. http://doi.org/10.1007/BF00713146

Su, Z., Timmermans, W. J., van Der Tol, C., Dost, R., Bianchi, R., Gómez, J. A., … Gillespie, A. (2009). EAGLE 2006 – Multi-purpose, multi-angle and multi-sensor in-situ and airborne campaigns over grassland and forest. *Hydrology and Earth System Sciences*, *13*(6), 833–845. http://doi.org/10.5194/hess-13-833-2009

Vesala, T., Rinne, J., Sogachev, A., Smolander, S., Markkanen, T., Foken, T., … Leclerc, M. Y. (2006). ON PRESENT FLUX FOOTPRINT MODELLING.

Vickers, D., & Mahrt, L. (1997). Quality control and flux sampling problems for tower and aircraft data. *Journal of Atmospheric and Oceanic Technology*. http://doi.org/10.1175/1520-0426(1997)014<0512:QCAFSP>2.0.CO;2

Wohlfahrt, G., Anderson-Dunn, M., Bahn, M., Balzarolo, M., Berninger, F., Campbell, C., … Cernusca, A. (2008). Biotic, Abiotic, and Management Controls on the Net Ecosystem CO2 Exchange of European Mountain Grassland Ecosystems. *Ecosystems*, *11*(8), 1338–1351. http://doi.org/10.1007/s10021-008-9196-2

Yang, X., & XingWang, M. (2001). Reviews of Several Aspects of Terrestrial Carbon Cycling. Advances in Earth Science.

Ying, H. (2005). Summary of Estimation Methods of the Carbon Stored in Forests. *World Forest Research*, *18*(1), 22–27.

Yu, H., & Huang, P. (2008). Carbon sink function of wetland: peatland and reed wetland cases. *Ecology and Environment*, *17*(5), 2103–2106.